

Modelling Thermal Insulation Effect of the Interface between Steel Deck and Concrete Slab in Composite Slab Systems in Fire Conditions

Varun Teja Vaddamani

A Dissertation Submitted to
Indian Institute of Technology Hyderabad
In Partial Fulfillment of the Requirements for
The Degree of Master of Technology



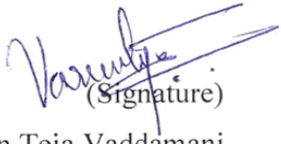
भारतीय प्रौद्योगिकी संस्थान हैदराबाद
Indian Institute of Technology Hyderabad

Department of Civil Engineering

July 2017

Declaration

I declare that this written submission represents my ideas in my own words, and where others' ideas or words have been included, I have adequately cited and referenced the original sources. I also declare that I have adhered to all principles of academic honesty and integrity and have not misrepresented or fabricated or falsified any idea/data/fact/source in my submission. I understand that any violation of the above will be a cause for disciplinary action by the Institute and can also evoke penal action from the sources that have thus not been properly cited, or from whom proper permission has not been taken when needed.



(Signature)

Varun Teja Vaddamani

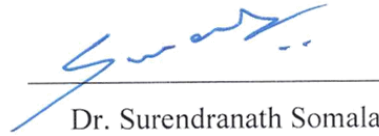
CE15MTECH11017

Approval Sheet

This thesis entitled “Modelling Thermal Insulation Effect of the Interface between Steel Deck and Concrete Slab in Composite Slab Systems in Fire Conditions” by Varun Teja Vaddamani is approved for the degree of Master of Technology from IIT Hyderabad.



Dr. Anil Agarwal
Assistant Professor, Civil Engineering
Adviser



Dr. Surendranath Somala
Assistant Professor, Civil Engineering
Examiner



Dr. Chandrika Prakash Vyasrayani
Associate Professor, Mechanical and Aerospace Engineering
Examiner

Acknowledgements

I sincerely thank Dr. Anil Agarwal, my project guide, and advisor, without whom this thesis would not have seen the light of the day. His constant encouragement and motivation helped me to gain insight knowledge in the project work. His ability to look at things in an all-round sense is always a source of inspiration, which reminds that knowledge gaining is a constant learning process.

I thank Mr. Hemanth Kumar Chinthapalli, my colleague, and friend, who helped me in times of need, despite his busy working schedule, and for giving valuable suggestions which are of immense help.

I thank my colleagues, Athira Ravindran, Banoth Kumari, for making this learning process enjoyable.

Dedicated to

My family,
whose constant encouragement, support and love
is the result of what I am today

Abstract

Steel-concrete composite slabs are gaining importance, due to the ease of construction without heavy lifting machinery and also the performance of steel decking as a permanent formwork and external reinforcement. At elevated temperatures, steel-concrete composite slabs experience debonding of steel deck from the concrete slab. This debonding creates a layer of air which offers thermal resistance to the rise of temperature in the concrete slab. There is very limited numerical or analytical work in the literature that provides a rational framework for thermal resistance offered by this intermediate layer. Experiment data to support the modelling research is also very sparse.

As a consequence of de-bonding of steel deck from the concrete slab, the heat transfer from the steel deck to the concrete slab is through radiation and conduction of the intermediate air layer. Preliminary structural analyses of the composite floor systems reported in the literature showed that a proper temperature calculation of the steel deck as well as concrete slabs is of great importance for the thermal gradient of the slab and thus for global load redistribution. The temperatures have a simultaneous effect on mechanical behaviour; and also the mechanical behaviour has a direct effect on temperatures, which can be understood through a fully coupled thermal-stress analysis. ABAQUS software is used for performing numerical simulations. However, there are certain limitations while defining the parameters of radiation.

The present work addresses a way to include the radiation effect due to debonding of steel deck in steel concrete composite slab, under standard fire conditions. The factors influencing the radiative heat transfer are studied in detail. As a first step, an uncoupled heat transfer analysis has been performed over a section of steel-concrete composite slab taking into account the radiation and conduction properties using interface elements. The radiation properties are accounted for, using equivalent conductance for the interface elements as a function of temperature. The concrete slab, the interface element and the steel deck are modelled using DC2D4 elements. Material properties for steel and concrete are adopted from Eurocode.

Contents

Declaration.....	ii
Approval Sheet	iii
Acknowledgements.....	iv
Abstract.....	vi
1 Introduction.....	1
1.1 Steel-Concrete Composite Slabs.....	1
1.2 De-bonding in Steel-Concrete Composite Slabs under high temperatures.....	1
1.3 Motivation behind the Study	2
2 Literature Review	4
2.1 Radiation: Introduction and Mathematical Definition.....	4
2.2 Heat Transfer and Boundary Conditions	5
2.3 Emissivity	6
2.4 View factor	7
2.5 Experimental and Numerical Research on steel concrete composite slabs	10
3 Objective and Scope	13
3.1 Research Motivation.....	13
3.2 Equivalent Conductance	14
3.3 Mathematical Formulation of Equivalent Conductance	14
3.4 First Methodology: Equation for Surface Temperature of Concrete	20
3.5 Second Methodology: Effective conductance vs. Temperature relation	22
4 Development of Numerical Model.....	27
4.1 Characteristics of the Numerical Model	27
4.2 Thermal Properties of Concrete at Elevated Temperatures	28
4.3 Specific Heat of Concrete.....	29
4.4 Thermal Conductivity of Concrete	30
4.5 Thermal Elongation of Steel.....	31
4.6 Specific Heat of Steel	32
4.7 Thermal Conductivity of Steel.....	33
4.8 Thermal Conductivity of Air	33

4.9	Thermal Expansion Coefficients of Concrete and Steel as per ASCE-78	34
4.10	Experimental Data for Validation.....	34
5	Results and Conclusions.....	37
5.1	Results: When radiation only is included	37
5.2	Results: When conductivity of air is considered along with Radiation	38
5.3	Results: Varying Emissivity of Steel	40
5.4	Results: TrayDec Slab	44
5.5	Results: Hibond Slab	47
5.6	Conclusions.....	51
	References.....	52

Chapter 1

Introduction

This chapter describes briefly about the steel-concrete composite slabs, the de-bonding effect of steel deck, and motivation behind the present study.

1.1 Steel-Concrete Composite Slabs

Steel Concrete Composite Slabs are used as roofs and floors to carry vertical loads in commercial structures such as buildings and bridges. They comprise of the concrete slab, which is cast on top of a flat/trapezoidal steel decking, and may include steel reinforcement along both the directions in the plane of the slab. Steel deck acts as permanent formwork for the concrete. The overall depth of slabs ranged from 100 mm to 150mm, with the height of steel deck from 45mm to 80mm and steel deck thickness ranging from 0.7mm to 1.5 mm. The profile of the steel deck can be flat, trapezoidal or re-entrant. For durability purposes, the steel deck is hot-dip galvanized. Indentation and embossments are used to improve the mechanical bond between the steel deck and the concrete slab. Main advantages of these composite slabs, as compared to the conventional reinforced concrete slabs are structural efficiency and speed of construction with ease.

1.2 De-bonding in Steel-Concrete Composite Slabs under high temperatures

When the bottom face of the slab is subjected to high temperatures, the steel deck is subjected to buckling and de-bonding from the bottom surface of the concrete. This occurs because the concrete, which was mechanically anchored to the concrete, gets

ripped off from the slab due to the release of steam. The steam releases because of the inherent moisture content present in the concrete slab.

When steel deck debonds from the concrete slab, it creates a layer of air between steel deck and concrete slab, which acts as a layer of insulation and therefore reduce the temperature rise at the bottom of the slab. Therefore, the temperature rise at the bottom of the slab is primarily due to phenomenon of convection and radiation from the heated steel deck, rather than the conduction through the steel deck. In most of the research work on the behaviour of structures at elevated temperatures, e.g. beams and columns, conduction phenomenon is the primary mode of heat transfer and most of the finite element packages such as ABAQUS have been very successful in performing thermal and stress analyses.

1.3 Motivation behind the Study

The motivation factor behind the study is to predict the concrete temperatures with reasonable accuracy, post debonding. Many researchers state that preliminary structural analyses of composite floor systems require proper temperature calculation in the concrete slab, and thus predict better fire resistance of the composite slab system. Till date, researchers focused on developing the fundamental understanding of composite slabs, and have come up with models calculating the load capacity of the composite slabs. Because of the evident debonding effect, the contribution of steel deck is not considered and this leads to a conservative estimate of strength of composite slabs at elevated temperatures. The steel deck, however, plays an important role in determining the temperature distribution within the concrete, and thereby affecting the overall fire resistance. It prevents the hot gases and flame during the fire event, reducing the heat flow into the concrete and controls spalling. This is an advantage over the conventional reinforced concrete slabs. Accurate prediction of concrete temperatures would be useful in evaluating correct fire resistance, thereby economizing the use of insulation.

The present work aims to propose an interface model, that can account for the thermal insulation of the interlayer between the steel deck and concrete slab.

Uncoupled heat transfer analyses are performed in ABAQUS using interface elements between steel deck and concrete slab. Detailed calibration and validation are used to find the appropriate thermal properties of the interface element, that account for the radiation and also the insulation effect between steel deck and concrete slab. As a consequence, an equation for predicting the surface temperature of concrete as a function of steel temperature is proposed which can evaluate the temperature distributions across the slab accurately.

Chapter 2

Literature Review

This chapter describes the factors influencing the radiation phenomenon in detail, and literature review of some experiments on steel-concrete composite slabs.

2.1 Radiation: Introduction and Mathematical Definition

Radiation is the phenomenon of heat transfer between two surfaces, or objects not in contact with each other. Unlike conduction and convection, which require a medium for heat transfer to take place, radiation can take place in vacuum. In most practical applications, all the three modes of heat transfer occur simultaneously, each mode with varying degrees of intensity.

Radiation is of two types: electromagnetic radiation and thermal radiation. Our interest is in thermal radiation, emitted as a result of energy transitions of molecules, atoms and electrons of a substance. At the microscopic level, the temperature is the measure of strength of these activities. In conduction and convection, the rate of heat transfer decreases with increasing temperature; whereas in thermal radiation, the rate of thermal radiation emission increases with increasing temperature. Thermal radiation is emitted by all the matter whose temperature is above absolute zero i.e. - 273 degrees centigrade. Thermal radiation is also defined as the portion of electromagnetic spectrum, that extends from about 0.1 to 100 μm i.e. it includes entire visible and infrared radiation, as well as a portion of ultraviolet radiation.

The amount of radiation energy emitted from a surface depends on the material of the body and the condition of the surface and the surface temperature. Therefore, different bodies emit different amounts of radiation per unit surface area, even when they are at same temperature. The maximum amount of radiation that can be emitted by a

surface, at a given temperature is expressed with reference to an idealized body, which is termed as a blackbody.

A blackbody is said to be a perfect emitter and absorber of radiation. A blackbody absorbs all incident radiation, and emits radiation energy uniformly in all the directions, per unit surface area, normal to the direction of emission.

The radiation energy emitted by a blackbody per unit time, per unit surface area was determined experimentally by Joseph Stephan in 1879 and expressed as

$$E_b(T) = \sigma T^4 \quad \left(\frac{W}{m^2} \right)$$

Where $\sigma = 5.67 \times 10^{-8} \left(\frac{W}{m^2 K^4} \right)$ is Stefan Boltzmann Constant and 'T' is the absolute temperature of the surface in Kelvin.

2.2 Heat Transfer and Boundary Conditions

Heat transfer takes place in three possible ways: Conduction, Convection and Radiation. Conduction deals with heat transfer within the solids. Convection deals with heat transfer by the movement of the medium (i.e. flow of air/liquid) around the solid body. Radiation is the transfer of heat via electromagnetic waves.

The heat conduction equation within a structural member is represented as

$$\lambda_x \frac{\partial^2 T}{\partial x^2} + \lambda_y \frac{\partial^2 T}{\partial y^2} + \lambda_z \frac{\partial^2 T}{\partial z^2} = \rho c \frac{\partial T}{\partial t}$$

where $\lambda_x, \lambda_y, \lambda_z$ are the thermal conductivities of the material in Cartesian coordinate directions x, y, z respectively; T is the temperature; t is the time; ρ is the density of the material, and c is the specific heat of the material.

To solve the above equation, heat transfer boundary conditions should be provided on the surface of the structural member, which is exposed to the fire environment. The boundary conditions in the form of convection and radiation boundary conditions are given as

$$\dot{h}_{net} = \dot{h}_{net,c} + \dot{h}_{net,r}$$

$$\dot{h}_{net,c} = \alpha_c(T_g - T_s), \quad \dot{h}_{net,r} = \phi \varepsilon_m \varepsilon_f \sigma [(T_g + 273)^4 - (T_s + 273)^4]$$

where $\dot{h}_{net,c}$, $\dot{h}_{net,r}$ are heat flux per area from convection and radiation respectively (in W/m²); T_g is the gas/fire temperature adjacent to the exposed surface; T_s is the surface temperature, α_c is the convective heat transfer coefficient (in W/m²-K); ε_m is the emissivity of the surface material, and ε_f is the emissivity of fire, usually taken equal to 1.0; $\sigma = 5.67 \times 10^{-8} \frac{W}{m^2-K^4}$ is the Stefan-Boltzmann Constant, and ϕ is the view factor or configuration factor. The important parameters which affect the radiation heat transfer, emissivity and view factor are discussed in the next section in detail.

2.3 Emissivity

The emissivity of a surface is defined as “*the ratio of radiation emitted by a surface at a given temperature to the radiation emitted by a blackbody at the same temperature*”. It is denoted by ε and it varies between zero and one. The emissivity of a material is a measure of how close a surface approximates a blackbody, for which $\varepsilon = 1$.

Hence, for a surface which is not a blackbody, the radiative energy per unit time per unit surface area can be expressed

$$E(T) = \sigma \varepsilon T^4 \quad \left(\frac{W}{m^2} \right)$$

Calculation of heat flux from radiation, which dominates most of the heat transfer process, requires understanding and careful evaluation of the emissivity in the radiation heat transfer coefficient for both steel and concrete. For steel, no consensus on the value of emissivity has been reached and various values have been proposed for adoption by different researchers. Swedish Institute of Steel Construction (SBI 1976) recommends a value of 0.8. Kay et al. (1996) tried to justify a value of 0.8 for emissivity of steel to be adopted. Eurocode 3 recommends a value of 0.7 for carbon

steel (CEN 2005). The usual practice has been to adopt a constant value of emissivity of steel to match experimental results, but Wong and Ghajel (2003a) reported that the steel emissivity varies with the temperature.

The emissivity of concrete is reported to be in the range of 0.63 to 0.94, depending on surface roughness, and type of concrete. Concrete with a rough surface has a higher emissivity than that of the concrete with a smooth surface. For the present study, the emissivity of concrete is taken to be 0.7 for all the cases.

In the case of composite slabs, the steel deck is galvanized (coated with zinc). During fire exposure, the galvanized coating starts oxidizing at a temperature of about 400°C. Research on determining the emissivity of steel states that emissivity increases upto 800°C and thereafter becomes constant.

Hence, for the present study the emissivity of the steel is considered as follows:

$$\varepsilon = \begin{cases} 0.28 & 0^{\circ}\text{C} \leq T_s \leq 400^{\circ}\text{C} \\ 0.28 + 0.00105T_s & 400^{\circ}\text{C} \leq T_s \leq 800^{\circ}\text{C} \\ 0.7 & T_s \geq 800^{\circ}\text{C} \end{cases}$$

2.4 View factor

Radiation heat transfer between surfaces depends on the orientation of the surfaces relative to one another, as well as their radiation properties and temperatures. View factor is defined as “*the fraction of radiation leaving one surface, that strikes another surface directly.*” It is a purely geometrical quantity and is independent of the surface properties and temperature.

As shown in the below figure, the view factor from surface 1 to surface 2 (denoted as F_{12}) can be calculated as

$$F_{12} = F_{A_1 \rightarrow A_2} = \frac{\dot{Q}_{A_1 \rightarrow A_2}}{\dot{Q}_{A_1}} = \frac{1}{A_1} \int_{A_1} \int_{A_2} \frac{\cos\theta_1 \cos\theta_2}{\pi r^2} dA_1 dA_2$$

where A_1, A_2 – areas of the oriented surfaces

θ_1, θ_2 - angles between the normal and the line connecting the surfaces 1 and 2 respectively.

r – Distance between the two elemental areas dA_1, dA_2

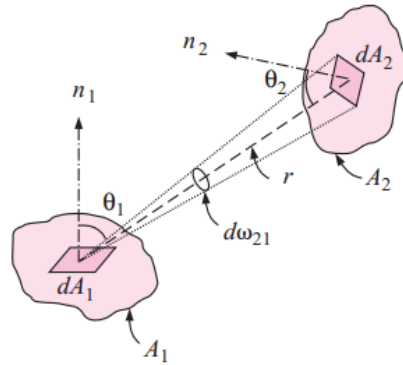


Figure 2.1 Geometry for the determination of view factor between two surfaces

The calculation of view factors obeys the reciprocity relation which states that

$$A_1 F_{12} = A_2 F_{21}$$

Also, most of the radiation phenomena in practice, involve enclosed spaces. The open spaces are also treated as imaginary surfaces with radiation properties equivalent to those of an opening. The conservation of energy principle states that the energy leaving any one surface of the enclosure must be intercepted by the other surfaces. Therefore, the sum of the view factors from a given surface 'i' of an enclosure to all the surfaces of an enclosure, including to itself must equal unity. This is commonly known as summation rule for an enclosure and is expressed as

$$\sum_{j=1}^N F_{i \rightarrow j} = 1$$

For composite slabs with flat sheeting, the view factor from the point of fire to the bottom of steel deck is generally taken as unity. For composite slabs with profiled/ re-entrant sheeting, it depends on the orientation of surfaces and the distance between them. Due to the obstruction from the web of steel deck (the inclined part of the

section), the view factors for the web and lower flange of steel deck are less than unity, which is adopted in Annex. G of EN 1991-1-2:2005.

The view factors for the upper flange and web portion of the steel deck are calculated using Hottel's Cross String Method and expressed as

$$\phi_{up} = \frac{ad + bc - ac - bd}{2ab} = \frac{\left(\sqrt{h_2^2 + \left(l_3 + \frac{l_1 - l_2}{2}\right)^2} - \sqrt{h_2^2 + \left(\frac{l_1 - l_2}{2}\right)^2}\right)}{l_3}$$

$$\phi_{web} = \frac{ac + cd - ad}{2ac} = \frac{\left(\sqrt{h_2^2 + \left(\frac{l_1 - l_2}{2}\right)^2} + (l_3 + l_1 - l_2) - \sqrt{h_2^2 + \left(l_3 + \frac{l_1 - l_2}{2}\right)^2}\right)}{2\sqrt{h_2^2 + \left(\frac{l_1 - l_2}{2}\right)^2}}$$

where ϕ_{up} , ϕ_{web} are the view factors for the upper flange and the web respectively and l_1, l_2, l_3, h_1, h_2 are the geometric parameters as described in the figure below

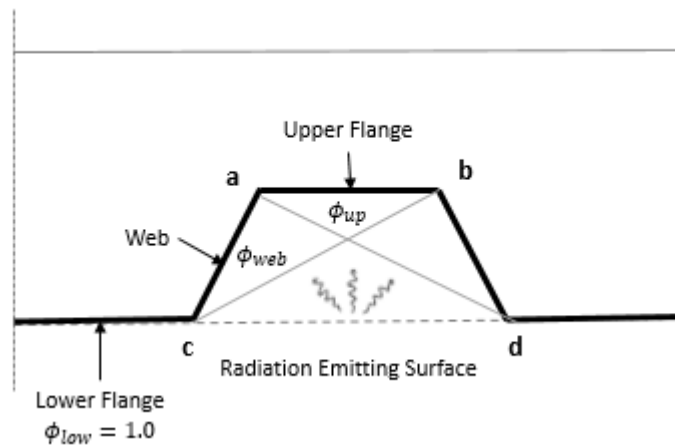


Figure 2.2 Schematic for Calculation of View factors for Steel Deck

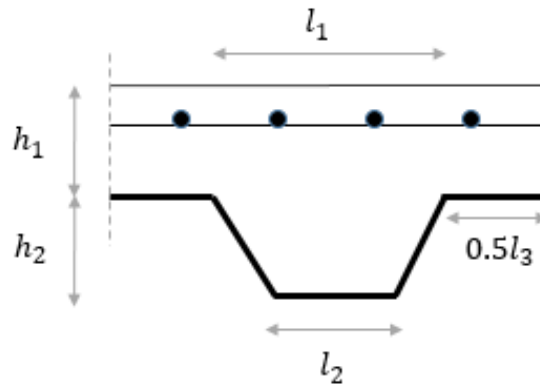


Figure 2.3 Geometric Parameters of Composite Slab

2.5 Experimental and Numerical Research on steel concrete composite slabs

Hammerlinck (1991) studied the behaviour of steel-concrete composite slabs at elevated temperatures. The aim of the study was to develop a mathematical model to analyse thermal and mechanical behaviour of fire exposed composite steel/concrete slabs. The models were verified on the basis of fire tests performed at Centre of Fire Research (TNO, Netherlands), as a part of an international research project, co-sponsored by European Coal and Steel Committee (ECSC). Twelve detailed test specimens were analysed to verify the thermal model, and six system test specimens were analysed to verify the mechanical model. Type of profiled sheet and the concrete depth were considered parameters for the study. Furnace temperatures in the experiments followed the standard ISO 834 curve.

Both (1998) performed four experimental tests on continuous two span composite slabs. Type of steel decking, reinforcement ratio, live load were the important parameters considered with respect to mechanical behaviour. Numerical modelling has been done for the experimental tests conducted as a part of ECSC research project. The slabs were subjected to furnace temperature, which followed the standard ISO 834 curve.

M.A.H. Halim et al. (1998) conducted fire tests on two steel concrete composite floor systems at University of Salford, UK. The aim of this study was to

develop fundamental information on behaviour of the composite steel concrete floor slabs. It is also reported that the fire resistance of the composite slab is greatly influenced by the steel deck, and though the contribution of steel deck is neglected in the calculation of fire resistance owing to its de-bonding effect, the debonding of steel deck influences the temperature distributions in the concrete slab, which in turn affect the overall fire resistance of composite slab.

Fire tests were conducted by Lim (2002) at the BRANZ Limited (New Zealand), in order to investigate the behaviour of unrestrained, simply supported, steel concrete composite slabs in a controlled furnace environment. The floor slabs consisted of three reinforced concrete plain flat slabs and three different composite steel-concrete slabs. Analytical design methods developed by researchers (Bailey, Clifton) are verified with the experimental results, along with numerical modelling of experiments using SAFIR finite element program. Linus Lim in his experiments has reported the debonding of steel deck from the concrete slab precisely. Numerical modelling of one of the composite slab has been done to validate the experimental observations using a special non-linear finite element program, SAFIR using shell elements. Two nonlinear finite element models for thermal and structural analysis respectively, are developed. The numerical results are observed to be higher than the experimental results. The reason can be attributed to the fact, that in his numerical modelling, the radiation effect due to de-bonding of steel deck has not been considered, and hence the numerical modelling reported higher values. However, it is also reported that the effect of de-bonding and the formation of air-gap can possibly be simulated with a 'fictitious' layer of thermal resistance.

As a part of the research project sponsored by CTICM France (2008), an 8.7m x 6.6 composite slab testing was performed, to provide an experimental evidence about composite slab behaviour subjected to standard ISO 834 fire, and to promote the design concept based on membrane action.

Bailey and Guo (2010) conducted a number of fire tests to investigate the behaviour of composite slab strips under both heating and cooling stages of fire. Different fire scenarios have been considered to study the thermal and mechanical behaviour due to

effect of different heating and cooling rates. A numerical study was followed to investigate the effect of steel deck thickness, the strength of concrete. It was observed that the influence of steel deck is significant in predicting the fire resistance of the composite slabs. Guo (2011) has proposed two separate nonlinear finite element models to simulate the thermal and structural analysis. In the thermal analysis model, 2D plane elements are adapted for steel, concrete and the interaction elements. In the structural analysis model, the concrete, the steel deck and reinforcement are modelled using solid, shell and truss elements respectively. The interaction between the steel deck and concrete was modelled using nonlinear spring elements. Debonding of steel deck is reported in the literature.

Four composite steel-concrete slabs, with trapezoidal steel decking were tested at Tongji University (2015). The aim of the study was to investigate the effect of presence of unprotected secondary beam, the direction of steel deck ribs, and the location of reinforcement. The slabs were subjected to ISO 834 curve for different durations of time, followed by a cooling phase until 180 min. Debonding of steel deck has been reported in the literature.

Chapter 3

Development of Modelling Technique

3.1 Research Motivation

The objective of this study is to develop an equation that can account for the radiation from the steel deck to the concrete slab, as well as the thermal insulation effect of the air gap during the debonding of steel deck in composite slabs. For the same, an ‘interface’ element is considered between the steel deck and the concrete, and the thermal properties of the interface element are defined through an ‘equivalent conductance’ relation as a function of temperature. The equivalent conductance takes into account the view factor effect, the emissivity of surfaces participating in radiation and the insulation effect due to the air gap.

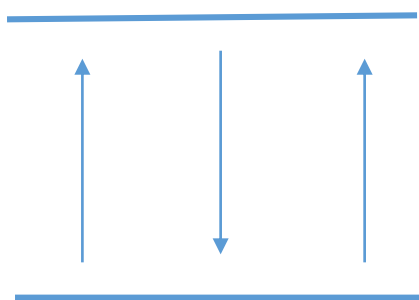


Figure 3.1 Radiation between two surfaces

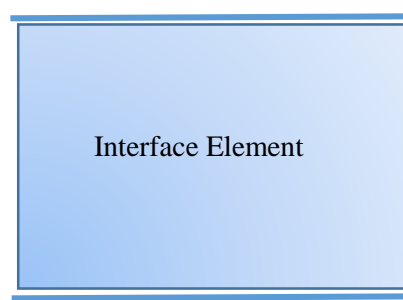


Figure 3.2 Equivalent conductance

3.2 Equivalent Conductance

During the fire test of composite slab, when the steel deck is subjected to fire, there is a continuous deformation of the steel deck in the form of buckling and debonding. The temperature has a direct effect on the mechanical behaviour of the system, and in return, the mechanical behaviour has an effect on the temperature. This implies that the structural and thermal behaviour are ‘coupled’ together. Hence, to capture the exact behaviour through numerical modelling, a ‘fully coupled thermal stress analysis’ is the only possibility to capture such effect. Though there is an option in ABAQUS to perform a fully coupled analysis, there are certain limitations. It is observed that view factor depends on the relative distance between the two surfaces, and also the orientation of the surfaces. ABAQUS limits the way of defining view factor as a function of relative distance or ‘clearance’ between the surfaces.

To overcome this limitation, an alternative to including the radiation effect and air gap insulation in the form of ‘equivalent conductance’ is chosen.

Thermal Conductance can be defined as “measure of the ability of a material to transfer heat energy per unit time, per unit surface area, and the temperature gradient through the thickness of the material.”

For a material with temperature gradient, where T_1 and T_2 are the high and low temperatures, across the thickness of the material, it can be mathematically expressed as

$$\dot{Q}_{eq} = h_c(T_1 - T_2)$$

Where h_c is the equivalent conductance of the material, accounting for radiation effect and conduction through the intermediate air layer.

3.3 Mathematical Formulation of Equivalent Conductance

Many researchers proposed different values of thermal conductance between steel and concrete elements. Ana Espinos has assumed a constant conductance value of 200 W/m²-K between the steel tube and concrete core in the thermal analysis of

elliptical CFT columns under fire. Guo and Bailey have assumed a constant conductivity of 0.8W/m-K for 1mm thickness of interaction element. Ghojel has proposed thermal conductance equations w.r.t temperature for loaded and unloaded square and circular CFT columns. Since the present work focuses on composite slab systems, and also the interaction between steel and concrete is different from the CFT columns, a different approach was employed for ‘thermal conductance’ calculation

The calculation of equivalent conductance is done through two steps. The first step comprises of evaluating the equivalent conductance from steel deck to concrete slab due to radiation only. The second step would be accounting for the conduction through the air gap. The assumptions made while calculating this parameter are 1) the steel deck debonds and deforms in the initial stages of the fire event, due to its very low thickness and high thermal strain developed because of temperature gradient between steel and concrete and 2) the steel deck debonds between the points of embedment and at points of embedment it is firmly locked into concrete slab.

Once the steel deck debonds, the heat transfers from steel deck to the concrete slab through radiation and conduction. For calculating the equivalent conductance due to radiation, consider two surfaces ‘1’ and ‘2’ temperatures T_1 and T_2 , with emissivities ε_1 and ε_2 , and the view factor from surface ‘1’ to surface ‘2’ be F_{12} .

The radiative flux between the two surfaces is given by

$$\dot{Q}_{rad} = F_{12}\sigma\varepsilon_{res}((T_1 + 273)^4 - (T_2 + 273)^4)$$

Where $\varepsilon_{res} = \frac{1}{\varepsilon_1} + \frac{1}{\varepsilon_2} - 1$ = Resultant Emissivity between surfaces

If it can be assumed that this radiative flux can be accounted by a material with equivalent conductance due to radiation h_{rad} , then we can represent the radiative flux due to equivalent conductance as

$$\dot{Q}_{rad} = F_{12}\sigma\varepsilon_{res}((T_1 + 273)^4 - (T_2 + 273)^4) = h_{rad}((T_1 + 273) - (T_2 + 273))$$

$$h_{rad} = \frac{F_{12}\sigma\varepsilon_{res}((T_1 + 273)^4 - (T_2 + 273)^4)}{((T_1 + 273) - (T_2 + 273))}$$

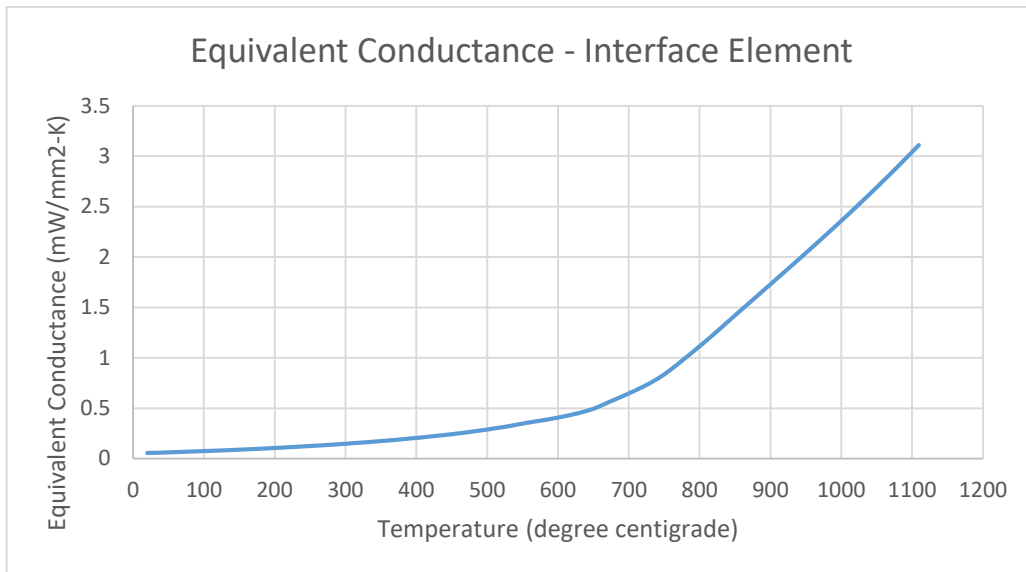


Figure 3.3 Graph of Equivalent Conductance due to Radiation

As shown in the Fig. 3.3 it can be inferred that the equivalent conductance is a cubic function of temperature.

The equivalent conductivity for a given thickness of an interface element is given by the relation

$$k_{int} = h_{rad}t_{int,rad} + k_{air}$$

where k_{int} is the total effective conductivity of the interface element, $t_{int,rad}$ is the thickness of the interface element considered, and k_{air} is the thermal conductivity of the air in the intermediate gap layer. The view factor between steel deck and concrete slab is taken equal to 1.0, assuming negligible heat loss due to debonding.

Two-dimensional radiative heat transfer analyses are performed in ABAQUS considering different thicknesses of interface element between steel deck and concrete slab. In most of the situations where the experiments are done on fire-exposed composite slabs, it is assumed that the temperature varies across the section in the longitudinal direction is constant. A representation of 2D mesh for concrete slab, steel deck and interface element, for a flat deck and a trapezoidal steel deck are shown in the below figure.

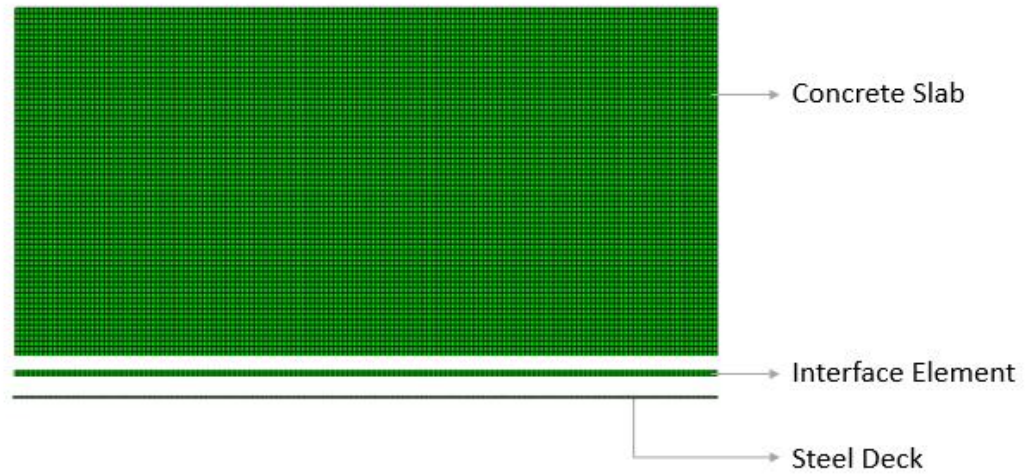


Figure 3.4 Representation of a 2D mesh for flat deck composite slab system

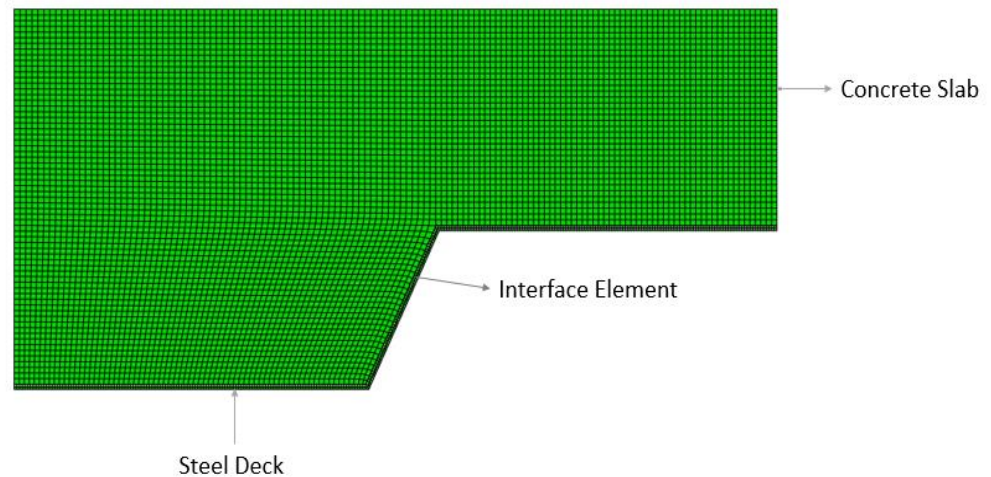


Figure 3.5 Representation of a 2D mesh for trapezoidal deck composite slab system

Thermal boundary conditions (convection and radiation) are given through the SFILM subroutine. As per the Eurocode specification, the convective heat transfer coefficient is taken to be $25 \text{ W/m}^2\text{-K}$ at the fire exposed surface, and $9 \text{ W/m}^2\text{-K}$ at the unexposed surface. The view factors for radiative heat transfer coefficient have been calculated as per the method described in Section 2.4 of Chapter 2. The variation of total

equivalent conductance with respect to the temperature of the steel deck for three different thicknesses of interface/gap is shown in the Fig. 3.4

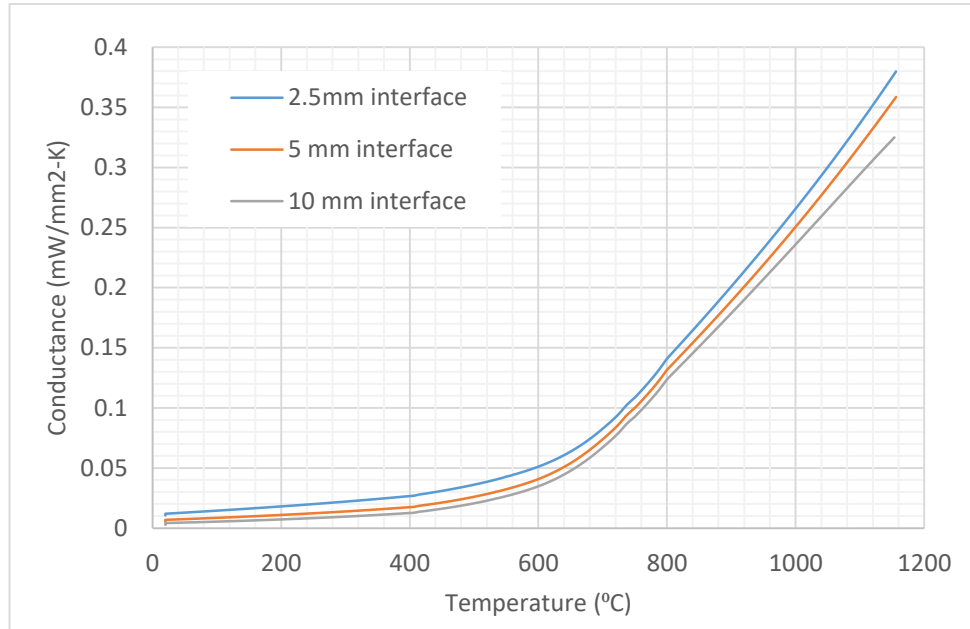


Figure 3.6 Total Equivalent Conductance w.r.t Temperature

The equivalent conductance relation is used to evaluate the total effective conductivity of the interface element. Using the interface element, 2D heat transfer analyses are performed to calculate the surface temperatures of the concrete slab. The thermal properties of the concrete slab and steel deck specimens are taken accordingly from the Eurocode provisions. The density and specific heat of the interface element are considered to be negligible since it is filled with the air gap due to heating up of inherent moisture from concrete slab. Specific cases were studied by varying the thickness of the interface element, ranging from 1 mm to 20 mm. One of the fire experiments performed by Lim has been adopted for understanding the effect of interface element. As mentioned in the experiments, the steel deck is subjected to a furnace temperature close to ISO 834. The temperatures of bottom surface of the concrete are plotted against the temperature of concrete when perfect contact is assumed. As shown in the below figure, when numerical analysis is performed assuming perfect contact, the temperature prediction of concrete surface is upto 200°C

higher than the experimental value. Hence, it is evident that the use of interface element improves the prediction of the surface temperature of the concrete slab.

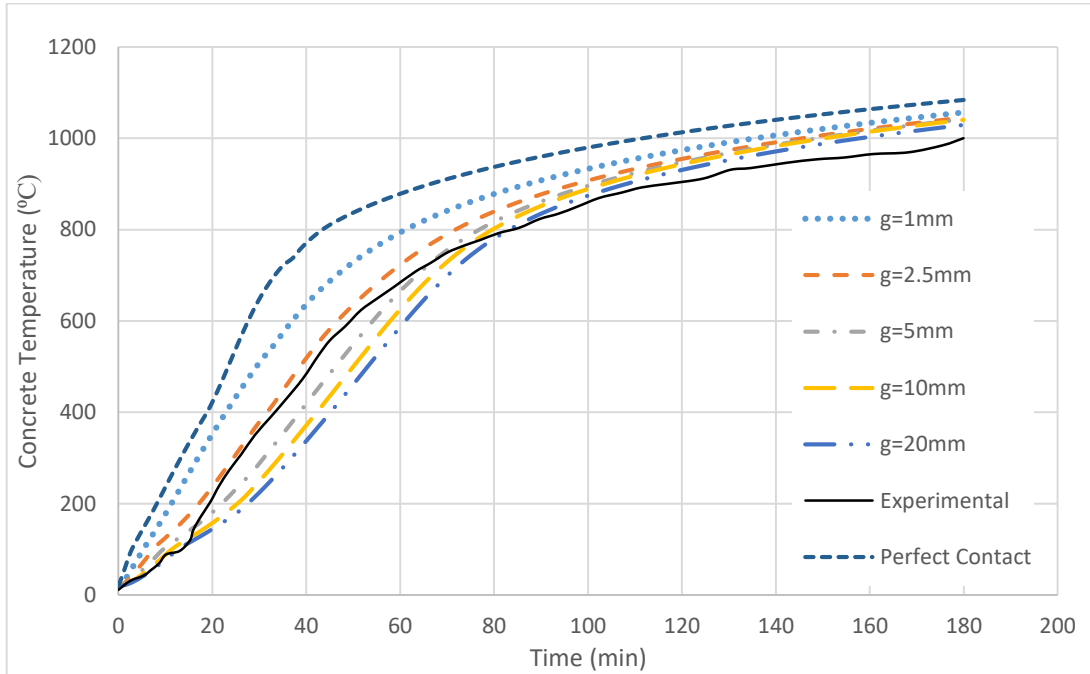


Figure 3.7 Temperature of bottom surface of concrete for various gaps

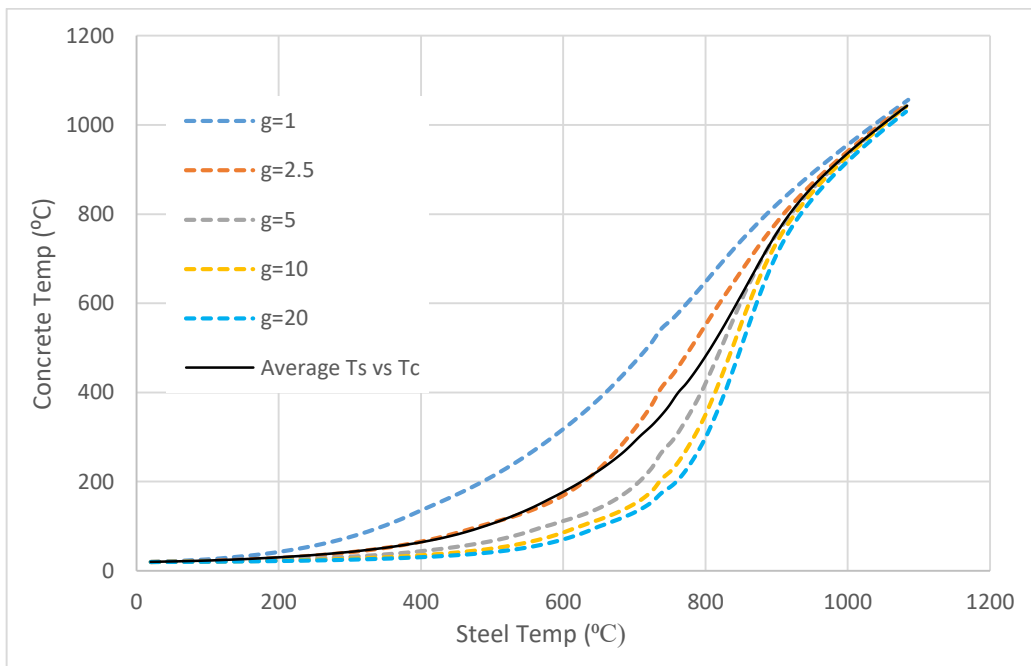


Figure 3.8 Concrete Temperature vs. Steel Temperature for various gaps

3.4 First Methodology: Equation for Surface Temperature of Concrete

In the first step, a simple but approximate methodology is adopted, where the effect of change of gap is not considered. Instead, an average value of all the curves of concrete temperature vs. steel temperature (Fig. 3.6) between 1 mm to 20 mm is taken. A relationship between the surface temperature of concrete and steel deck is formulated as shown in below equation.

$$T_c = \begin{cases} \frac{T_s^2}{2060} + 0.3T_s + 20 & T_s \leq 400^\circ C \\ \frac{T_s^2}{840} - 0.8T_s + 350 & 400^\circ C \leq T_s \leq 800^\circ C \\ -\frac{T_s^2}{320} + 7.715T_s - 3700 & 800^\circ C \leq T_s \leq 1200^\circ C \end{cases}$$

The above equation accounts for the effect of gap in an averaged sense, and the input is steel temperature T_s during a ‘perfect contact’ analysis (here interface element is not used).

The surface temperature of concrete is expressed in terms of the ISO 834 standard furnace temperature as

$$T_c = \begin{cases} \left(\frac{T_g}{127}\right)^3 - \left(\frac{T_g}{70}\right)^2 + 0.07T_g + 20 & T_g \leq 600^\circ C \\ \left(\frac{T_g}{80}\right)^3 - \left(\frac{T_g}{25}\right)^2 + 0.3T_g + 70 & 600^\circ C \leq T_g \leq 800^\circ C \\ \left(\frac{T_g}{19}\right)^2 - 2.16T_g + 240 & 800^\circ C \leq T_g \leq 900^\circ C \\ -\left(\frac{T_g}{48}\right)^3 + 0.02T_g - 10.65T_g + 520 & 900^\circ C \leq T_g \leq 1100^\circ C \end{cases}$$

Following are the results of the surface temperature of concrete as per the above equation in comparison to perfect contact case:

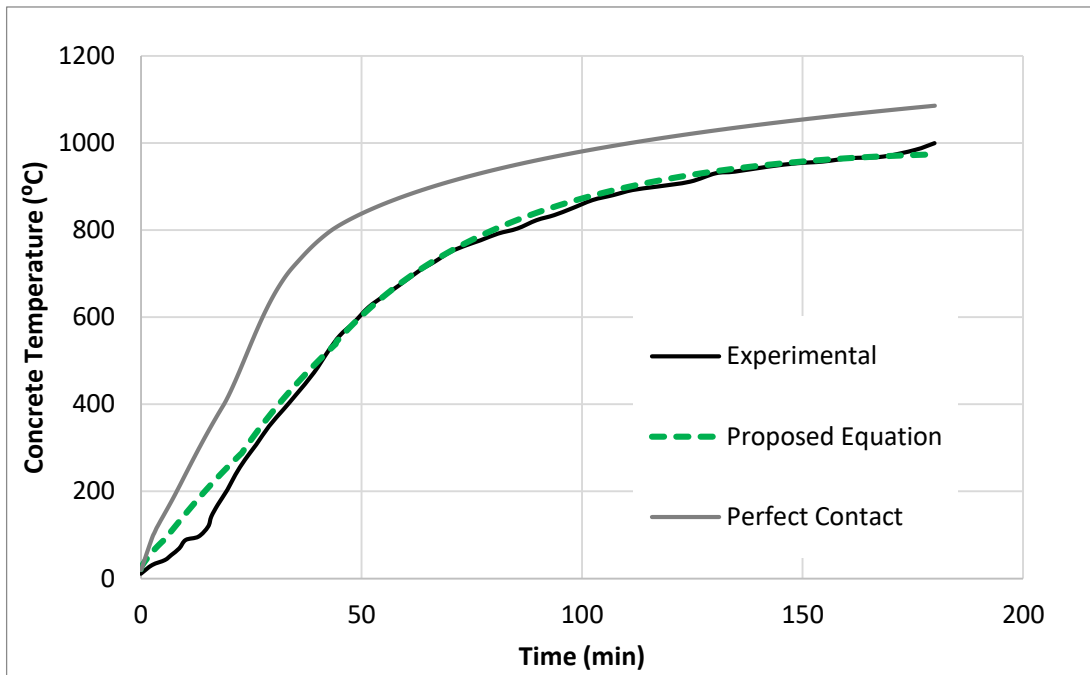


Figure 3.9 Temperature of Concrete Surface as per proposed equation - TrayDec Slab

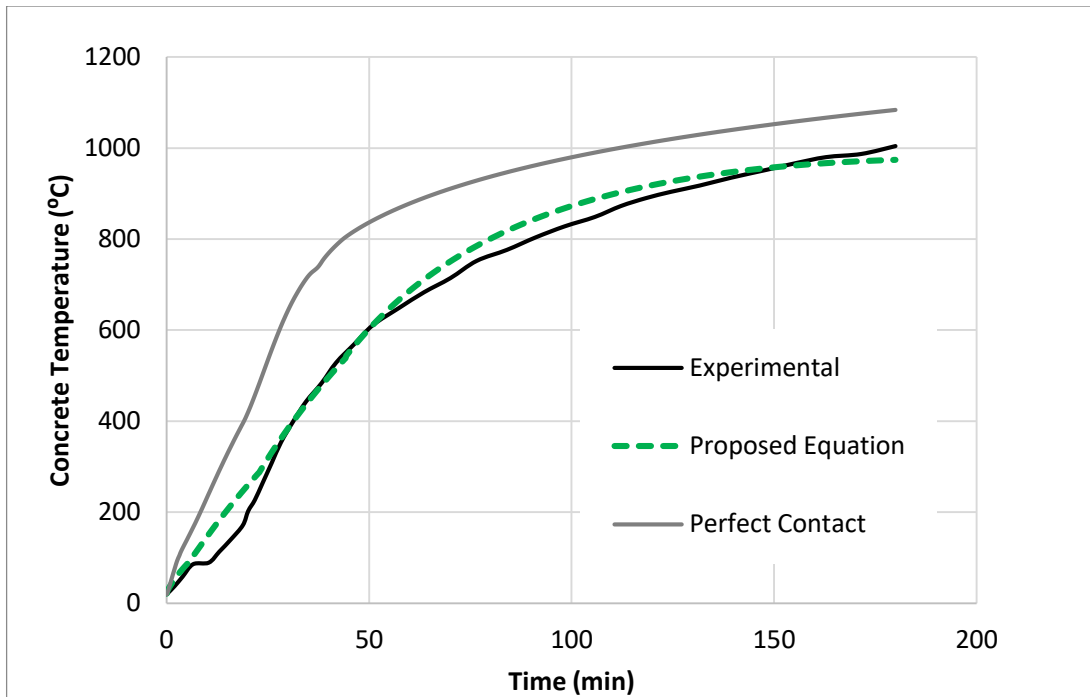


Figure 3.10 Temperature of concrete surface as per proposed equation - Hibond Slab

3.5 Second Methodology: Effective conductance vs. Temperature relation

It must be noted that the above results are for a constant value of gap during one analysis. However, in real experiment scenario, the gap value keeps increasing due to thermal gradient between steel deck and concrete slab. Hence, a more accurate and realistic phenomenon is needed to calculate the concrete temperatures, taking into account the thermal insulation effect. A second methodology is proposed in detail in this section.

Variation of this gap is a function is a function of thermal expansion coefficient and also the distance between points of embedment of steel deck. The steel deck is embedded into concrete at points of embossments/corrugations depending on the profile of the slab. However, it varies between 150 mm to 300 mm in most of the practical cases.

To understand how gap varies with the thermal gradient between steel deck and concrete slab, a simple calculation of thermal strains in concrete slab and steel deck is done. The time-temperature curves of concrete and steel, the distance between the points of embedment are the input parameters. The gap due to deformation of steel deck is assumed to be of a parabolic profile, for a flat deck. This assumption renders that the evaluation of the gap, in this case, is purely a geometrical calculation. In a real experiment, it is really difficult to say how the gap varies between steel deck and concrete slab after debonding.

Following is the procedure for calculating the gap values due to the thermal gradient between steel and concrete, for which the time temperature curve for the steel deck and concrete slab is known.

Step 1 : The temperature-time history of steel deck and concrete slab T_c, T_s is known. The length of embedment of the steel deck and concrete slab at ambient temperature is known. At ambient temperature, there is no expansion observed in steel and concrete.

Step 2 : As the temperature rises beyond ambient temperature, steel and concrete start expanding. Due to different thermal expansion coefficients (α_{steel} being higher than $\alpha_{concrete}$ during initial rise of temperatures), and the steel is assumed to be firmly locked between points of embedment, deformation of steel w.r.t concrete surface is observed. The thermal expansion coefficients are adopted from ASCE codes.

Step 3 : Thermal strains, and thermal elongations are calculated i^{th} point of time, for both steel and concrete where $i = 1$ to n , ($n =$ no. of time steps of thermal analysis) as

$$\begin{aligned}\epsilon_{c,i} &= \alpha_{c,i} \Delta T_{c,i} = \alpha_{c,i} (T_{c,i} - T_{ambient}), & \epsilon_{s,i} &= \alpha_{s,i} \Delta T_{s,i} = \alpha_s (T_{s,i} - T_{ambient}) \\ l_{c,i} &= s_{conc} (1 + \epsilon_{c,i}), & l_{s,i} &= s_{steel} (1 + \epsilon_{s,i})\end{aligned}$$

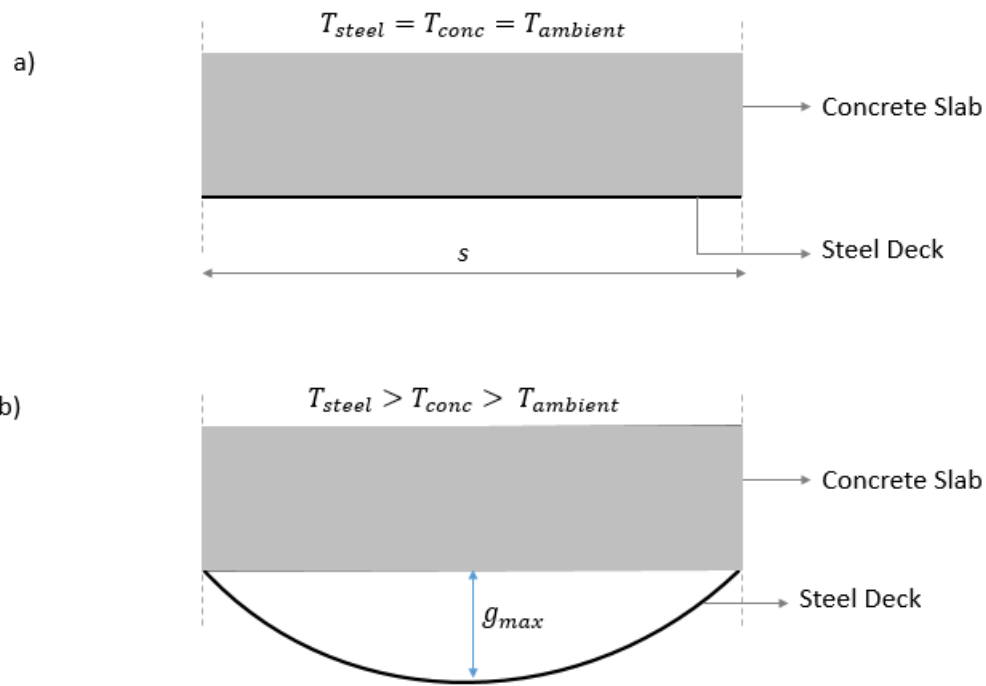


Figure 3.11 Representation of gap formation due to thermal gradient

a) at ambient temperature b) other than ambient temperature

Step 4 : To calculate the gap formation, the steel deck is assumed to deform in a parabolic profile given by the equation

$$y = g_{max} \left(1 - \frac{4x^2}{s^2} \right) \quad -\frac{s}{2} \leq x \leq \frac{s}{2}$$

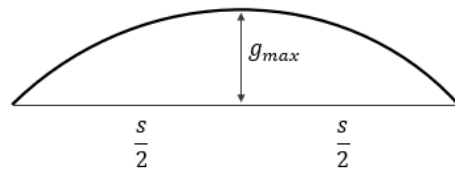


Figure 3.12 Profile of a parabola

The amount of maximum gap formed at a given time is calculated from the below equation

$$l_{s,i} = \sqrt{\frac{l_{c,i}^2}{4} + 4g_{max}^2} + \frac{l_{c,i}}{8g_{max}} \sin^{-1}\left(\frac{4g_{max}}{l_{c,i}}\right)$$

Using above procedure, the variation of maximum gap w.r.t the steel temperature for different lengths of embedment are shown in below figure.

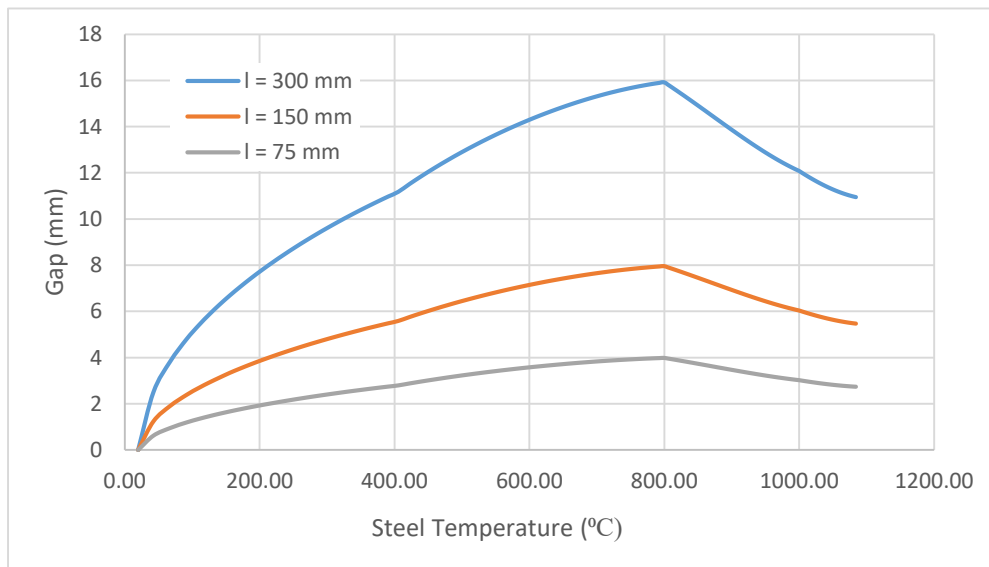
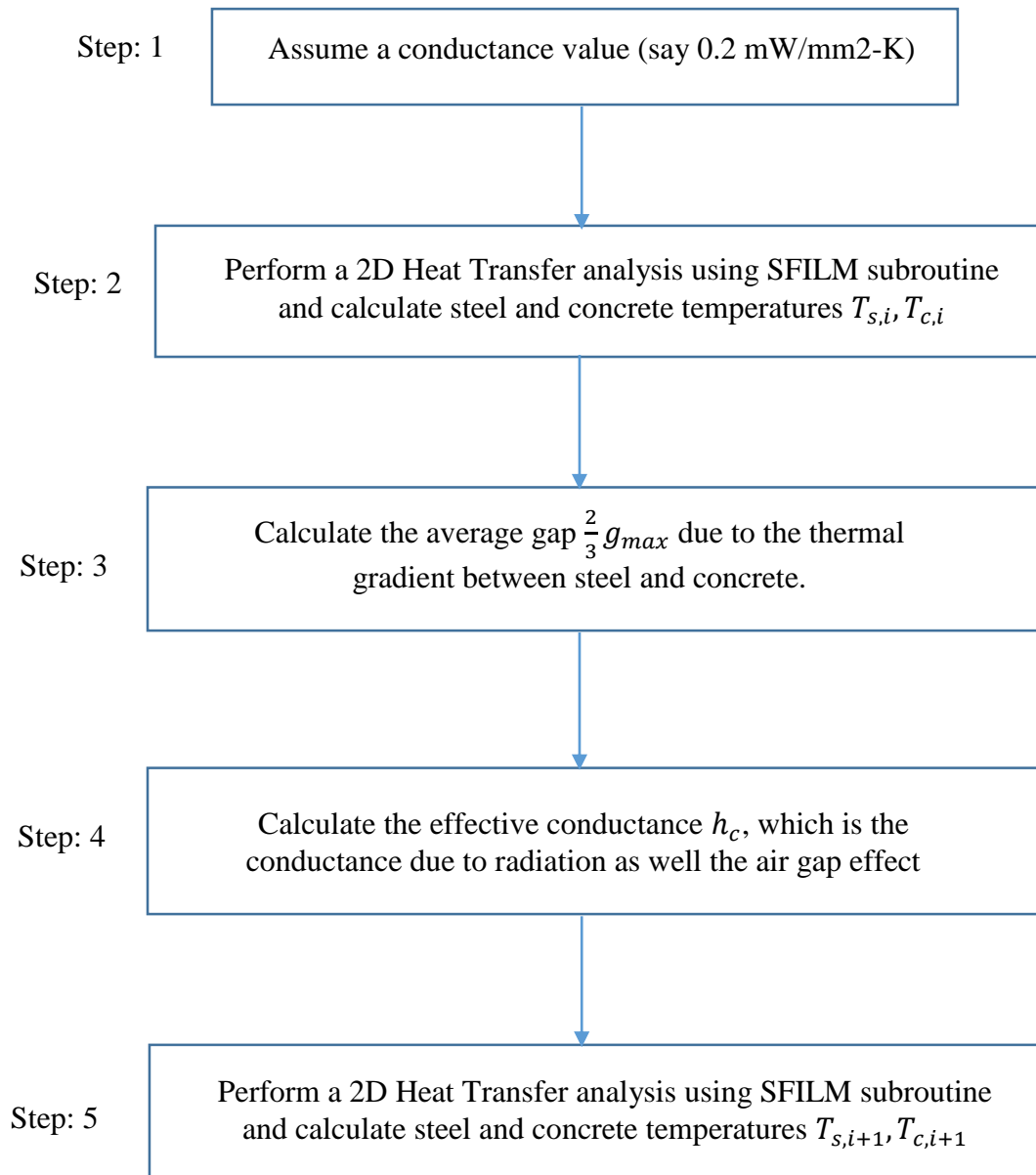


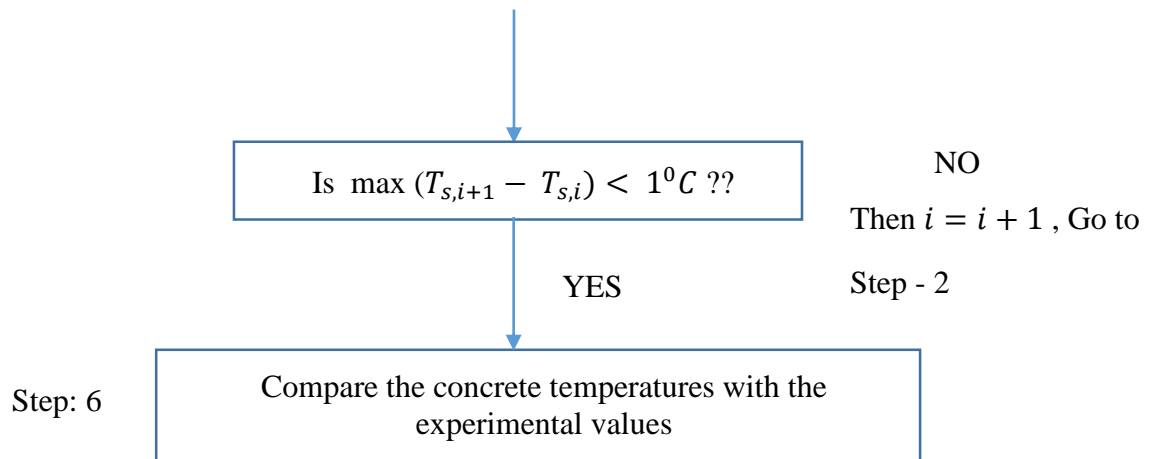
Figure 3.13 Variation of gap between steel deck and concrete slab

From the above discussion, it is evident that the parameters affecting the gap are concrete and steel temperatures, the length between points of embedment of steel deck. This gap, in turn, affects the distribution of concrete temperature.

The steel temperature is observed to have a steady increase up to a certain temperature (approximately up to 700 degrees) and then shows a nearly stable behaviour in the increase of temperature. Hence, the gap between steel and concrete increases as long as there is a temperature difference between steel and concrete. From this understanding, an iterative approach to evaluate the effective conductance as a function of temperature is proposed. The iterations are performed until there is no subsequent increase in the temperature of steel. The procedure is explained through a flowchart given below:

FLOWCHART





From the above iterative procedure, we obtain a point where the gap due to steel temperature and concrete temperature difference, gets stabilized. The effective conductance is that value of conductance for which the gap variation stabilizes, or remains constant after any iteration from this point.

Chapter 4

Material Properties and Experimental Data for Validation

This chapter presents the complete description of the finite element model developed for modelling the radiation and thermal insulation effect of debonding in the composite slabs. Results from the numerical model are validated against the fire tests available in the literature. Emissivity is varied to study the change in behaviour.

4.1 Characteristics of the Numerical Model

A two dimensional, plane numerical model for uncoupled heat transfer analysis is developed. The main parameters are the width of the section (W), depth of section (D), the thickness of the steel deck (t). The interface element of a certain thickness is used between steel deck and concrete slab. The bottom of steel deck is subjected to a time-dependent temperature curve, ISO 834 given by

$$T(t) = 20 + 345 \log_{10}(8t + 1) \text{ where } t = \text{time duration in minutes}$$

For the 2D analysis, the steel deck, interface element, and the concrete slab are modelled using DC2D4 elements. In the 3D analysis, DC3D8 elements are used for concrete, DS4 elements are used for steel, and DC1D2 elements are used for reinforcement. In most situations involving fire-exposed composite slabs, the temperatures are assumed to vary only across the thickness of the section, and are uniform across the length of the slab.

4.2 Thermal Properties of Concrete at Elevated Temperatures

Thermal Elongation of Concrete

The thermal strain of the concrete $\varepsilon_c(\theta)$ may be determined from the following with reference to the length at 20°C :

Siliceous Aggregates:

$$\varepsilon_c(\theta) = -1.8 \times 10^{-4} + 9 \times 10^{-6}\theta + 2.3 \times 10^{-11}\theta^3 \quad \text{for } 20^{\circ}\text{C} \leq \theta \leq 700^{\circ}\text{C}$$

$$\varepsilon_c(\theta) = 14 \times 10^{-3} \quad \text{for } 700^{\circ}\text{C} < \theta \leq 1200^{\circ}\text{C}$$

Calcareous Aggregates:

$$\varepsilon_c(\theta) = -1.2 \times 10^{-4} + 6 \times 10^{-6}\theta + 1.4 \times 10^{-11}\theta^3 \quad \text{for } 20^{\circ}\text{C} \leq \theta \leq 805^{\circ}\text{C}$$

$$\varepsilon_c(\theta) = 12 \times 10^{-3} \quad \text{for } 805^{\circ}\text{C} < \theta \leq 1200^{\circ}\text{C}$$

Where θ is the temperature of the concrete in degrees centigrade.

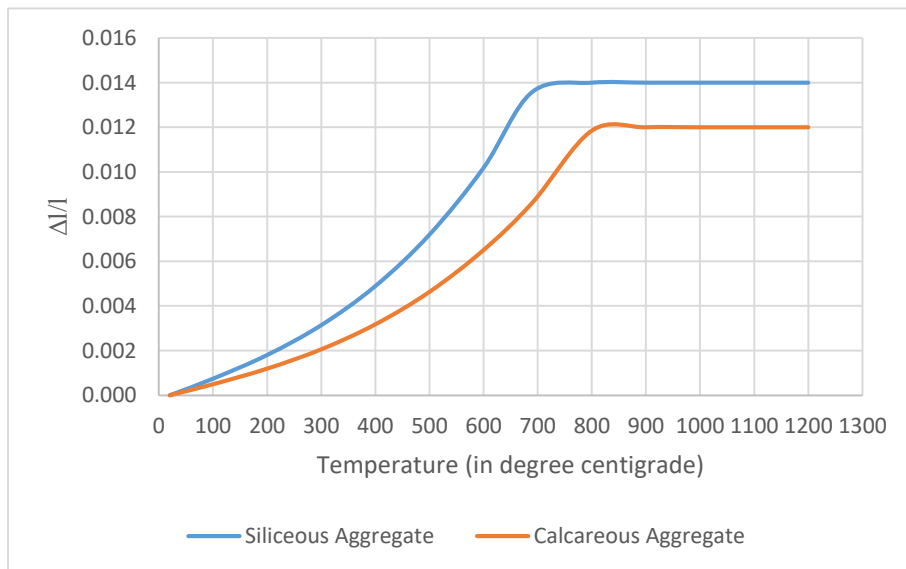


Figure 4.1 Variation of Thermal Elongation of Concrete with Temperature

4.3 Specific Heat of Concrete

The specific heat of dry concrete (in J/kg-K) may be determined from the following equations:

$$\begin{aligned}c_p(\theta) &= 900 && \text{for } 20\text{ }^{\circ}\text{C} \leq \theta \leq 100\text{ }^{\circ}\text{C} \\c_p(\theta) &= 900 + (\theta - 100) && \text{for } 100\text{ }^{\circ}\text{C} < \theta \leq 200\text{ }^{\circ}\text{C} \\c_p(\theta) &= 1000 + 0.5 * (\theta - 200) && \text{for } 200\text{ }^{\circ}\text{C} < \theta \leq 400\text{ }^{\circ}\text{C} \\c_p(\theta) &= 1100 && \text{for } 400\text{ }^{\circ}\text{C} < \theta \leq 1200\text{ }^{\circ}\text{C}\end{aligned}$$

The moisture content effect for 3% and 10% is included in numerical analysis within temperature range of 100 °C – 200 °C , with a constant peak at 115 °C by accounting for additional capacity as shown. For intermediate values, linear interpolation is recommended.

At 3% and 10%, peak value of specific heat = 2020 J/kg-K and 5600 J/kg-K respectively

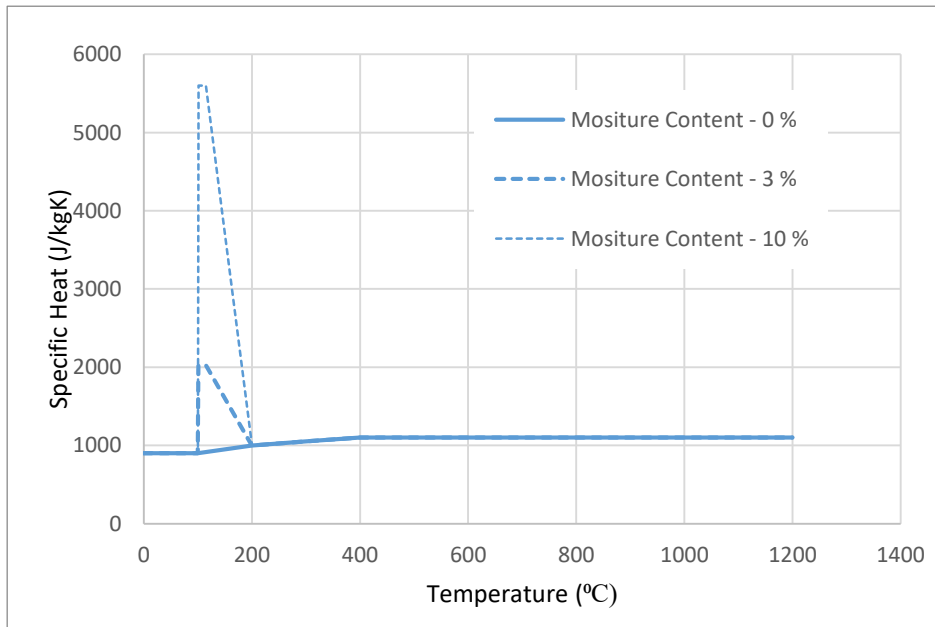


Figure 4.2 Specific Heat of Dry Concrete

4.4 Thermal Conductivity of Concrete

Upper limit of thermal conductivity λ_c (in W/m-K) of normal weight concrete may be determined from the following equation:

$$\lambda_c = 2 - 0.2451 \left(\frac{\theta}{100} \right) + 0.0107 \left(\frac{\theta}{100} \right)^2 \quad \text{for } 20^\circ\text{C} \leq \theta \leq 1200^\circ\text{C}$$

Where θ is the concrete temperature.

Lower limit of thermal conductivity λ_c (in W/m-K) of normal weight concrete may be determined from the following equation:

$$\lambda_c = 1.36 - 0.136 \left(\frac{\theta}{100} \right) + 0.0057 \left(\frac{\theta}{100} \right)^2 \quad \text{for } 20^\circ\text{C} \leq \theta \leq 1200^\circ\text{C}$$

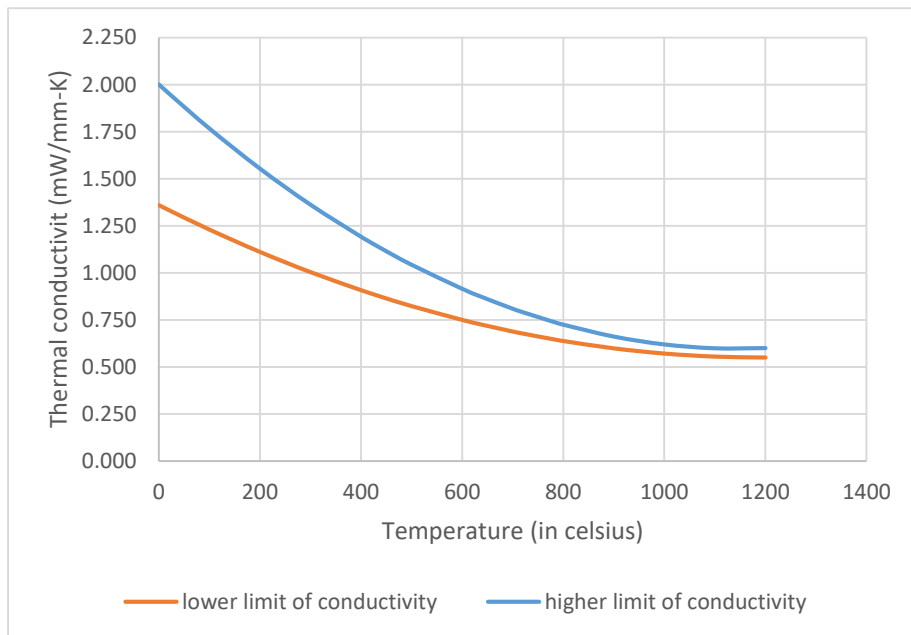


Figure 4.3 Thermal Conductivity of Concrete

4.5 Thermal Elongation of Steel

Thermal elongation of steel $\Delta l/l$ shall be determined from the following :

$$\frac{\Delta l}{l} = 1.2 \times 10^{-5} \theta_a + 0.4 \times 10^{-8} \theta_a^2 - 2.416 \times 10^{-4} \quad \text{for } 20^\circ\text{C} \leq \theta \leq 750^\circ\text{C}$$

$$\frac{\Delta l}{l} = 1.1 \times 10^{-2} \quad \text{for } 750^\circ\text{C} < \theta \leq 860^\circ\text{C}$$

$$\frac{\Delta l}{l} = 2 \times 10^{-5} \theta_a - 6.2 \times 10^{-3} \quad \text{for } 860^\circ\text{C} < \theta \leq 1200^\circ\text{C}$$

Where θ_a is the steel temperature in degree centigrade

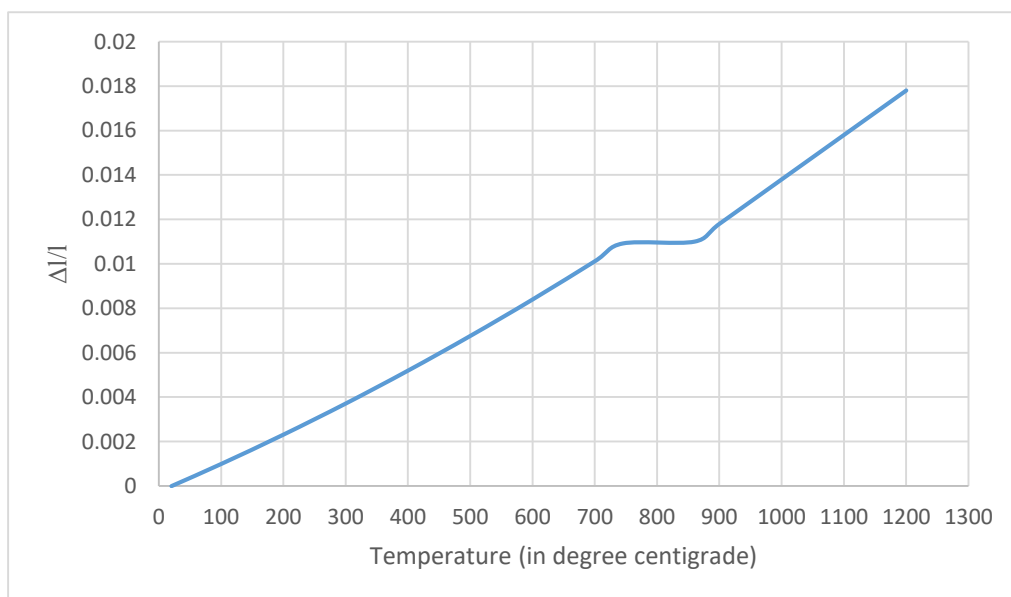


Figure 4.4 Thermal Elongation of steel

4.6 Specific Heat of Steel

Specific Heat of Steel c_a (in J/kg-K) shall be calculated as follows :

$$c_a = 425 + 7.73 \times 10^{-3} \theta_a - 1.69 \times 10^{-3} \theta_a^2 + 2.22 \times 10^{-6} \theta_a^3 \quad 20^\circ\text{C} \leq \theta_a \leq 600^\circ\text{C}$$

$$c_a = 666 + \frac{13002}{738 - \theta_a} \quad \text{for } 600^\circ\text{C} \leq \theta_a < 735^\circ\text{C}$$

$$c_a = 545 + \frac{17820}{\theta_a - 731} \quad \text{for } 735^\circ\text{C} \leq \theta_a < 900^\circ\text{C}$$

$$c_a = 650 \quad \text{for } 900^\circ\text{C} \leq \theta_a \leq 1200^\circ\text{C}$$

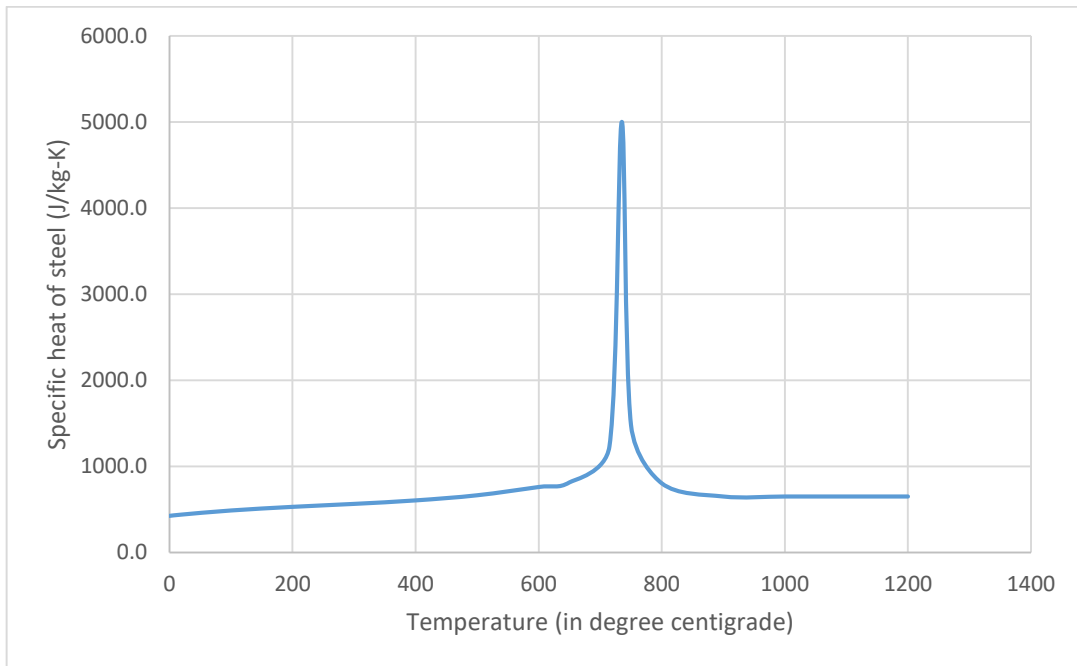


Figure 4.5 Specific Heat of Steel

4.7 Thermal Conductivity of Steel

Thermal Conductivity of Steel λ_a (in W/m-K) shall be calculated from the following equation :-

$$\lambda_a = 54 - 3.33 \times 10^{-2} \theta_a \quad \text{for } 20^\circ\text{C} \leq \theta_a < 800^\circ\text{C}$$

$$\lambda_a = 27.3 \quad \text{for } 800^\circ\text{C} \leq \theta_a \leq 1200^\circ\text{C}$$

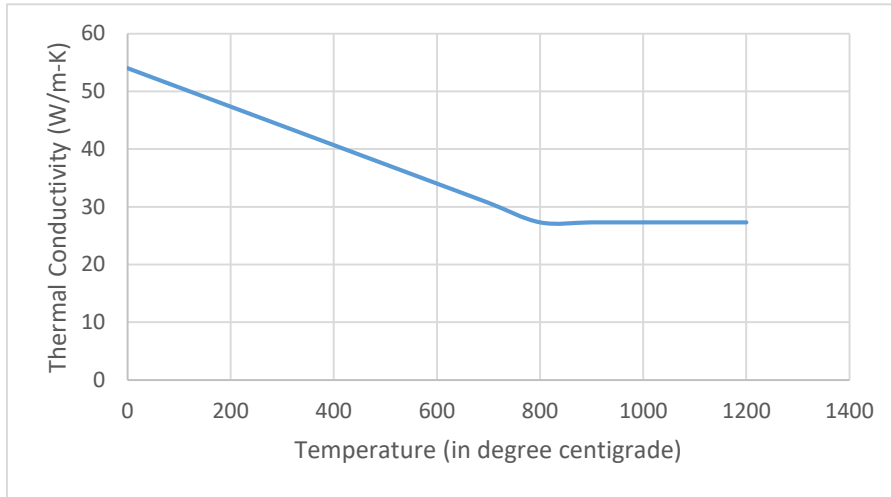


Figure 4.6 Thermal Conductivity of Steel

4.8 Thermal Conductivity of Air

Thermal conductivity of air w.r.t temperature is shown below. For intermediate values of temperature, interpolation is made.

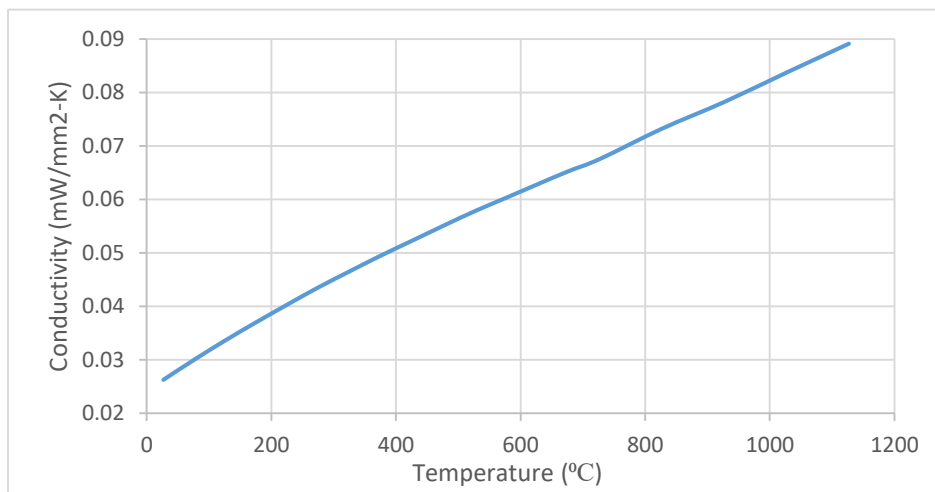
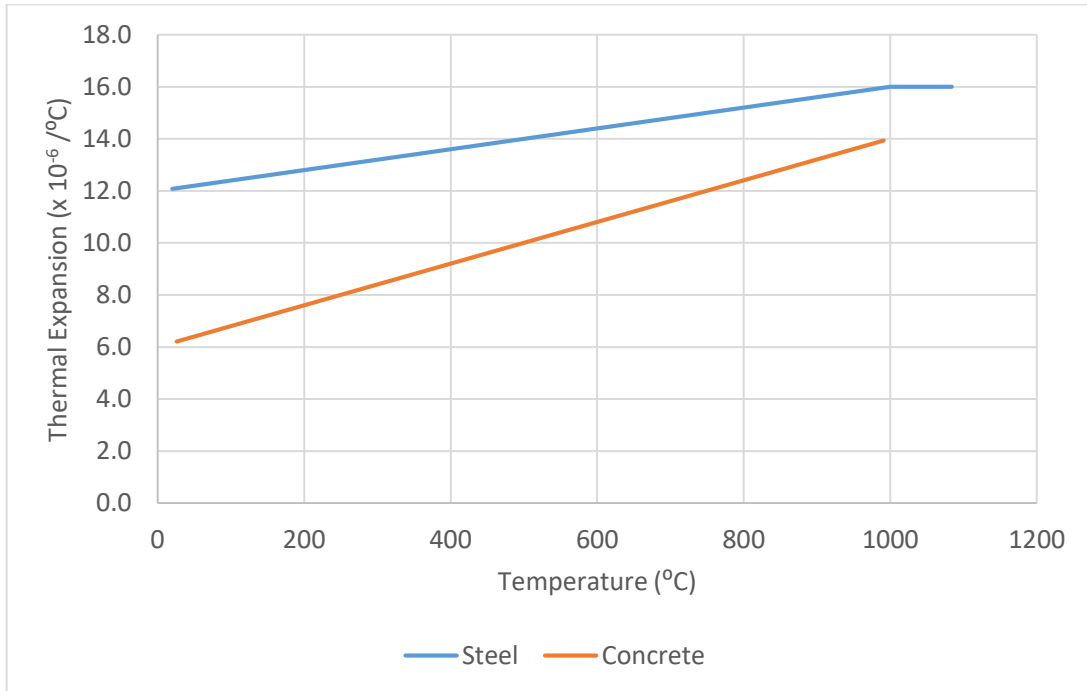


Figure 4.10 Thermal Conductivity of Air 1

4.9 Thermal Expansion Coefficients of Concrete and Steel as per ASCE-78

The thermal expansion coefficients from ASCE-78 are used for the second methodology (as described in Chapter 3).



4.10 Experimental Data for Validation

Uncoupled 2D heat transfer analyses are performed in ABAQUS. The experimental data has been taken from Lim. (2002). Flat slab and trapezoidal steel deck types are taken for validation. The experimental data used for validation are subjected to a furnace temperature that follows the standard ISO 834 curve. The summary of the experiments done is given below:

1) Flat Deck Profile:-

Composite Slab	TrayDec
Dimensions of the slab	4.3 m x 3.3 m
Slab Thickness	130 mm
Compressive Strength of Concrete (28 days)	30.2 MPa
Thickness of steel deck	0.75 mm
Yield Strength of structural Steel	550 MPa
Reinforcing Steel	8.7 mm dia @ 300 mm c/c – Two way spanning
Yield Strength of Reinforcing Steel	565 MPa
Mositure Content(by weight)	5.1 %

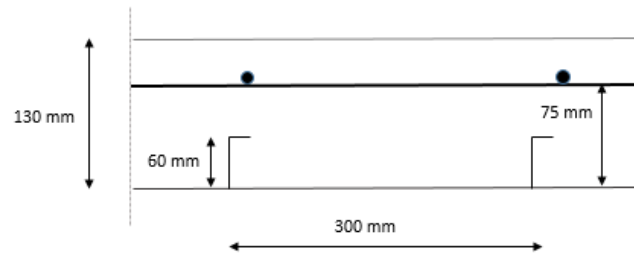


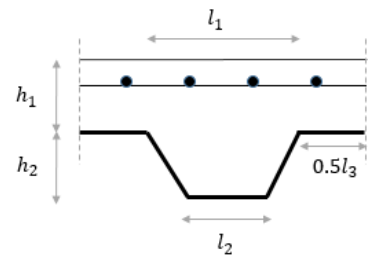
Figure 4.11 TrayDec Slab Section

2) Trapezoidal Profile :-

Composite Slab	Hibond
Dimensions of the slab	4.3 m x 3.3 m
Concrete Slab Thickness	130 mm
Compressive Strength of Concrete (28 days)	30.2 MPa
Thickness of steel deck	0.75 mm
Yield Strength of structural Steel (at 20 °C)	550 MPa
Reinforcing Steel	8.7 mm dia @ 300 mm c/c – Two way spanning
Yield Strength of Reinforcing Steel	565 MPa
Mositure Content(by weight)	5.1 %

Geometric Properties of the trapezoidal sections (dimensions in mm)

Decking	h ₁	h ₂	l ₁	l ₂	l ₃
Hibond	75	55	182	130	126



Chapter 5

Results and Conclusions

The temperatures obtained after the heat transfer analysis were measured at various locations starting from the bottom of the concrete surface. 2D heat transfer analyses without interface elements are performed, to confirm the fact that the temperatures are over predicted when the radiation effect and thermal insulation of air gap are not considered. To validate the proposed hypothesis, heat transfer analyses with and without interface elements are performed using the two methodologies described in Chapter 3, for the available experimental data.

5.1 Results: When radiation only is included

The steel deck bottom surface has the input temperature. Comparison between the surface temperature of concrete when interface element is not used, and when interface element is used is given below. Only radiation is taken into account through equivalent conductance in the below-represented results.

The figure below shows, that the results of numerical analysis are higher than the experimental results, thereby indicating that due to debonding of steel deck, the contact is lost, and the temperature rise is no more due to conduction, but due to radiation. Also, the steam generated in between the concrete slab and steel deck, creates a thermal layer of insulation, preventing the temperature rise in concrete.

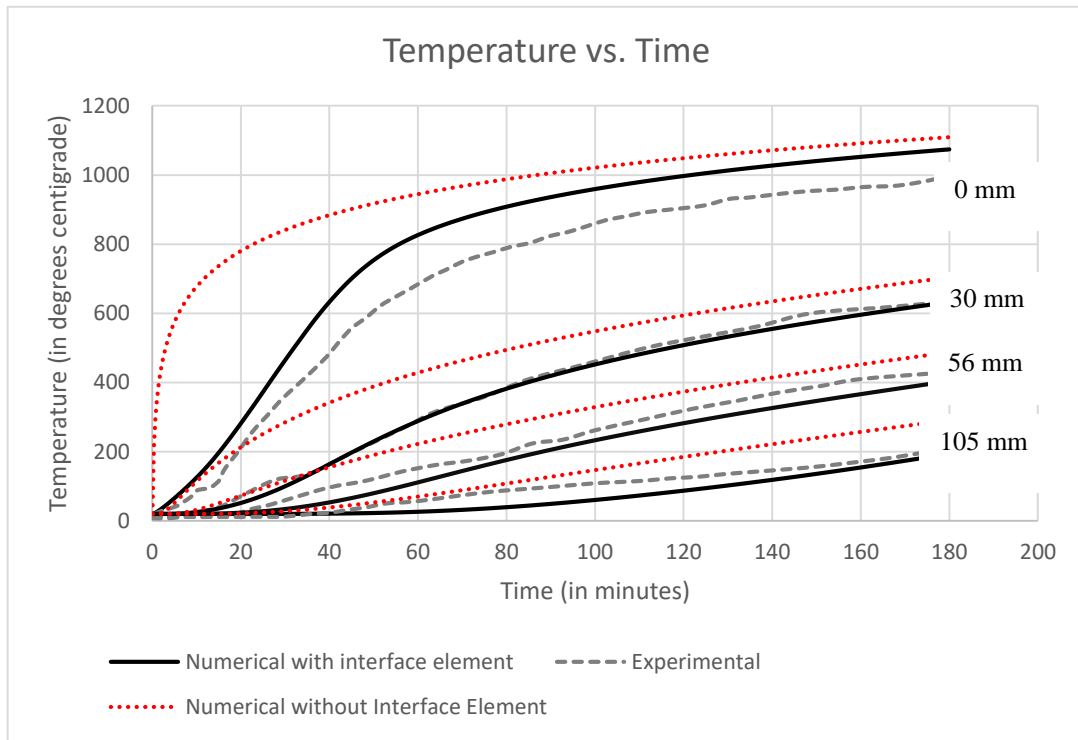


Figure 5.1 Temperatures across the concrete section

5.2 Results: When conductivity of air is considered along with Radiation

A similar heat transfer analysis is performed, including the inherent conductivity of air along with the radiation in the equivalent conductance of the interface material. It is observed that when conductivity of air is included, the numerical results reported even higher temperatures.

It is to be noted that, even when the interface element is used, the temperature predictions are higher than the experimental results, but not as high as when there is a perfect contact between steel and concrete. The same is depicted in the Fig.5.1 and Fig. 5.2. Hence, radiation effect has to be considered while performing numerical analyses of composite slabs, which exhibit debonding behaviour.

Also, the variation in temperature of bottom surface is plotted, when only equivalent conductance and when equivalent conductance along with conductivity of air is used, in Fig.5.3

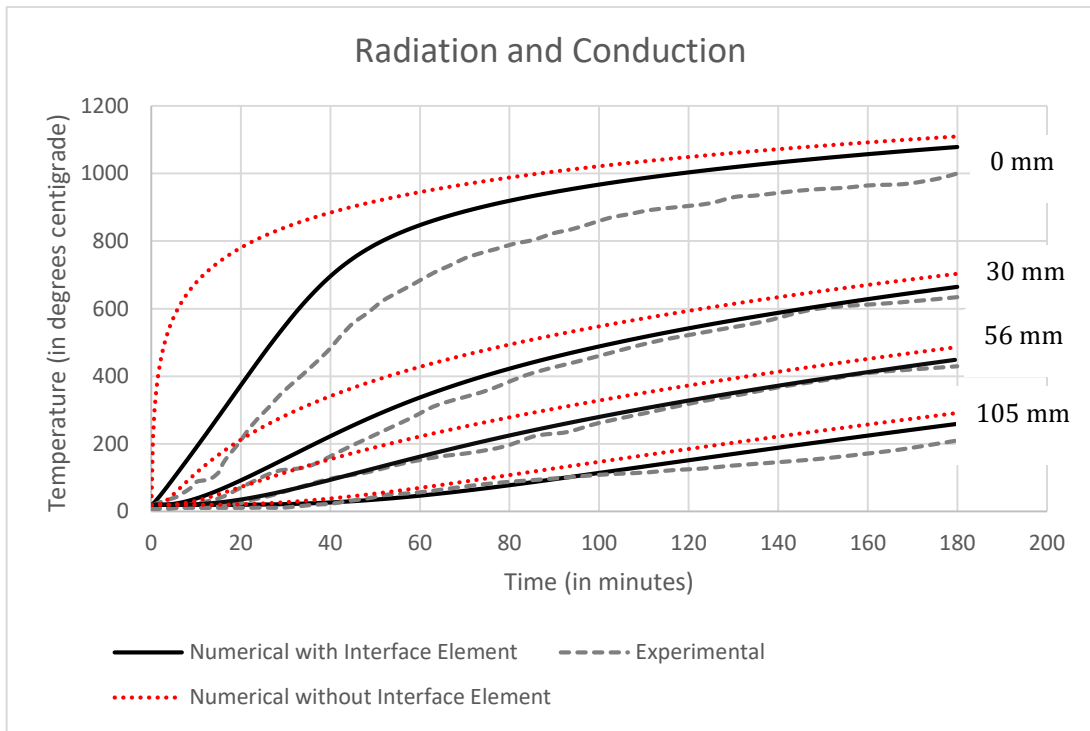


Figure 5.2 Temperatures across the concrete section

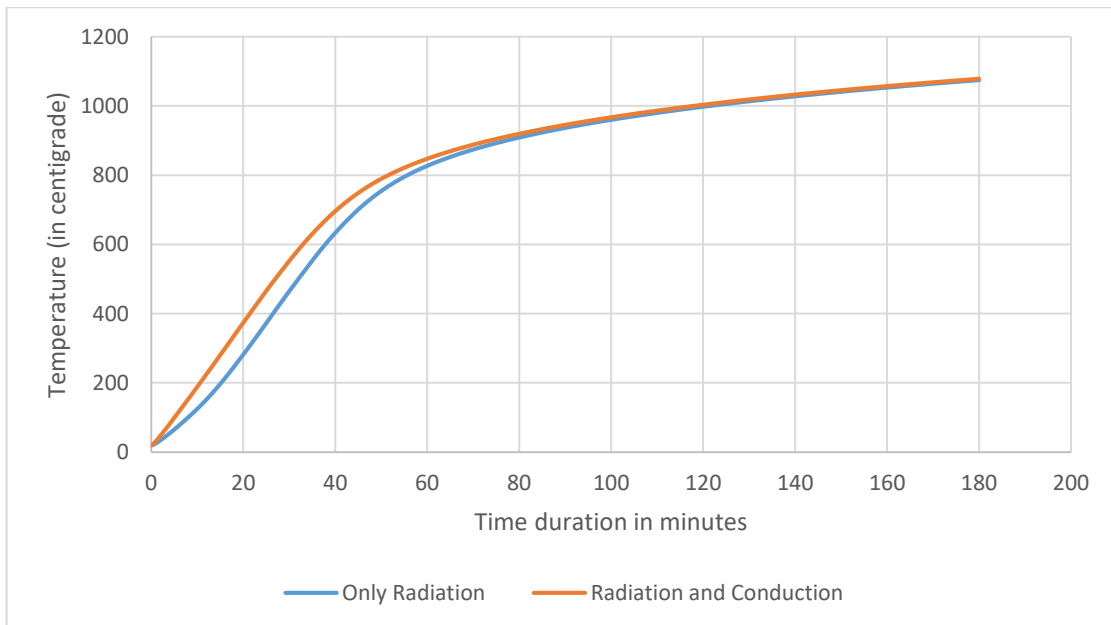


Figure 5.3 Temperature variation at the bottom surface of concrete section

In the experiments conducted by Linus Lim, it is reported that the steel deck bends in double curvature. Since the slab is simply supported at both the ends, there was hardly any opening into the atmosphere which caused significant heat loss i.e. all the radiative flux from the steel is incident on concrete, irrespective of the magnitude of deflection of steel deck, and orientation of the steel deck. Hence, the view factor from the steel deck to the concrete slab is assumed to be equal to unity.

5.3 Results: Varying Emissivity of Steel

Apart from the view factor, emissivity of steel has an impact on the radiative flux from the steel surface. Hence, a range of values of emissivity varying from 0.3 to 0.7 has been selected, and the heat transfer analysis was run for each case of emissivity, considering the conductivity of air along with the equivalent conductance. The results at bottom surface of the concrete, and at a point 30mm from the surface are shown below:

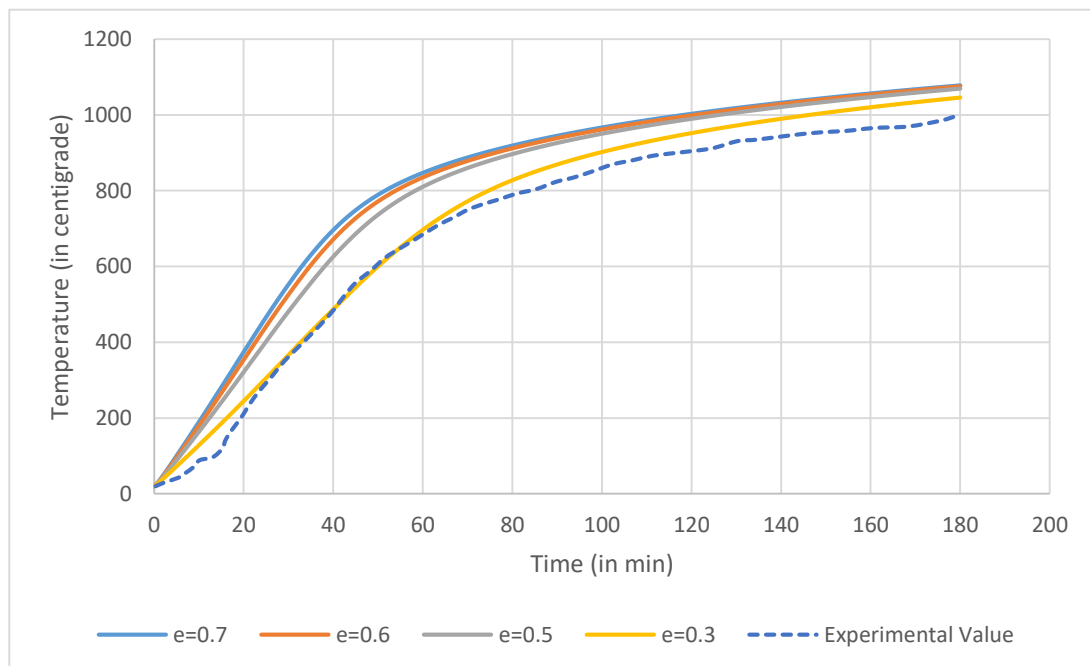


Figure 5.4 Temperatures at bottom surface of concrete

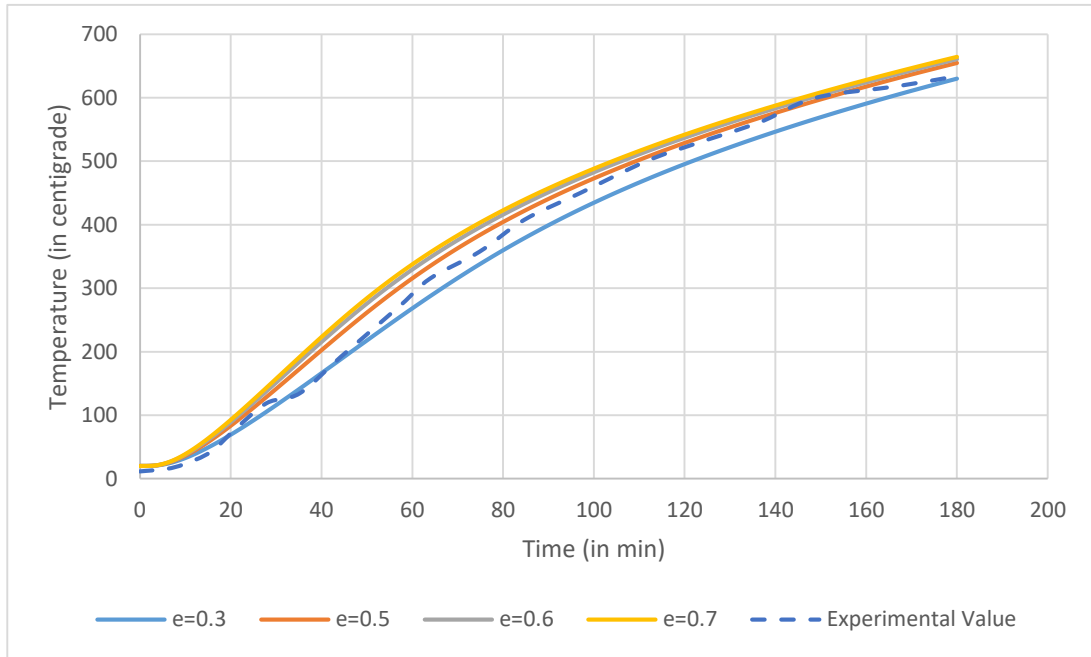


Figure 5.5 Temperature at 30mm above the concrete surface

Similarly, for a given emissivity value of steel, the temperatures across different points on the concrete section are plotted, which are shown below

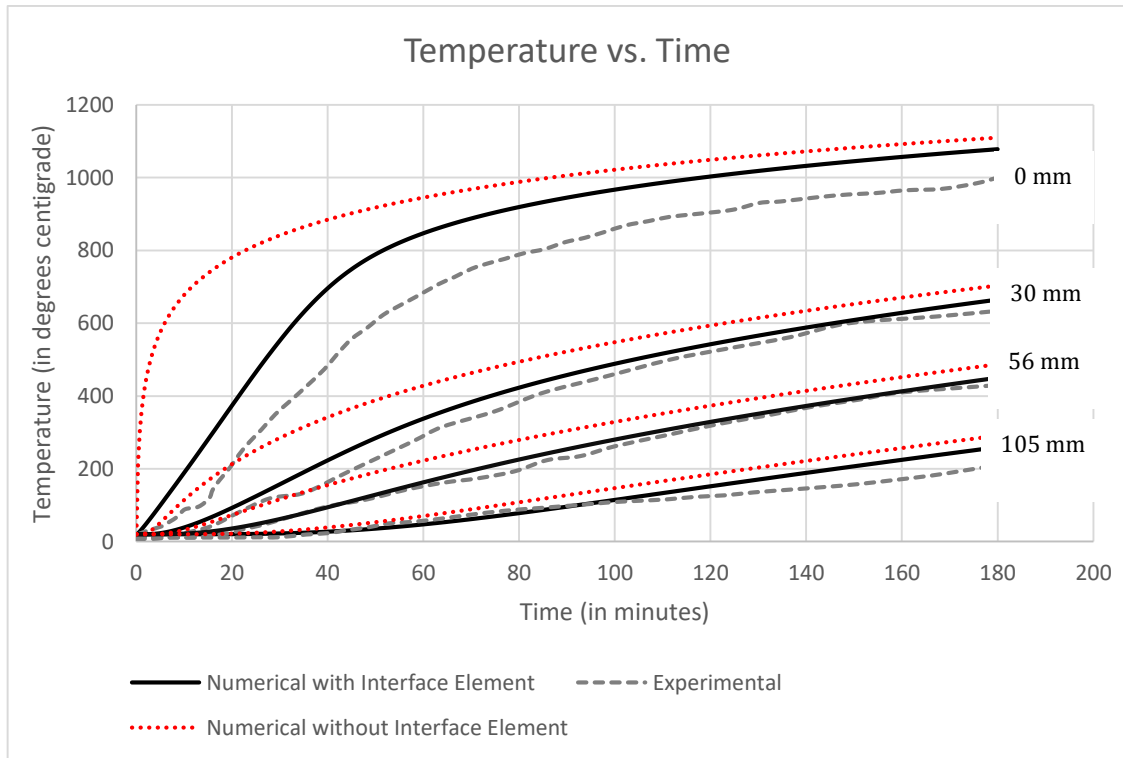


Figure 5.6 Temperature distribution for emissivity of steel as 0.7

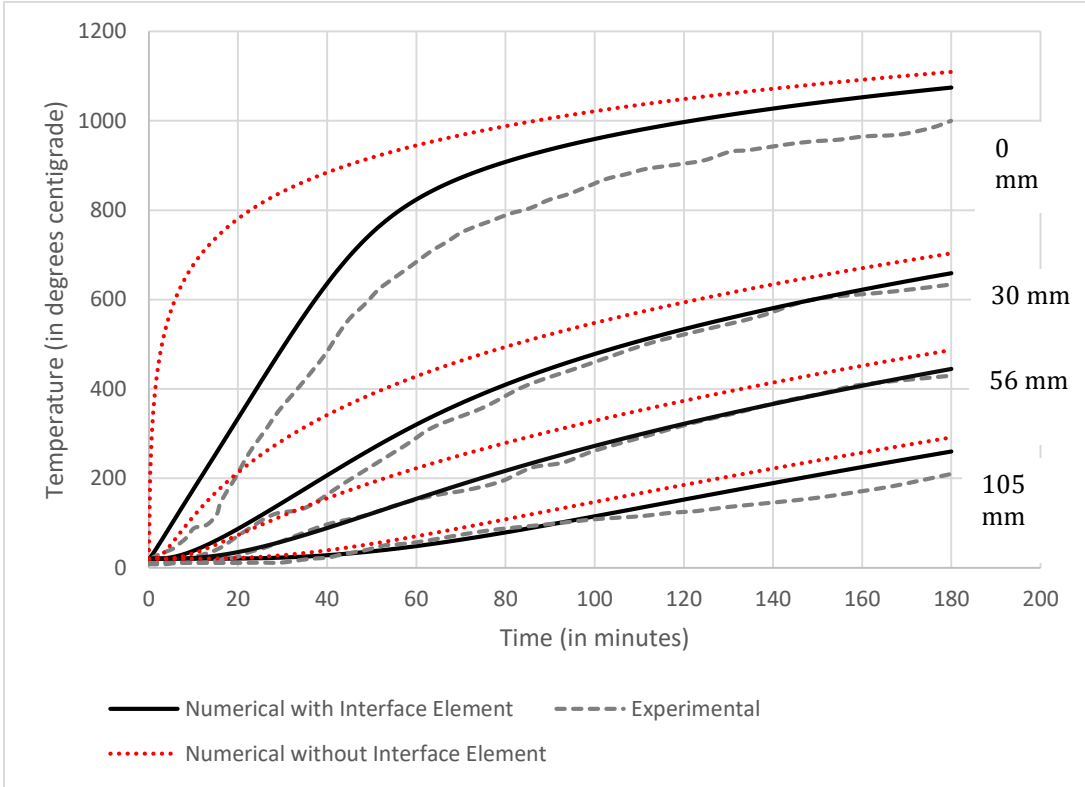


Figure 5.7 Temperature distribution for emissivity of steel as 0.6

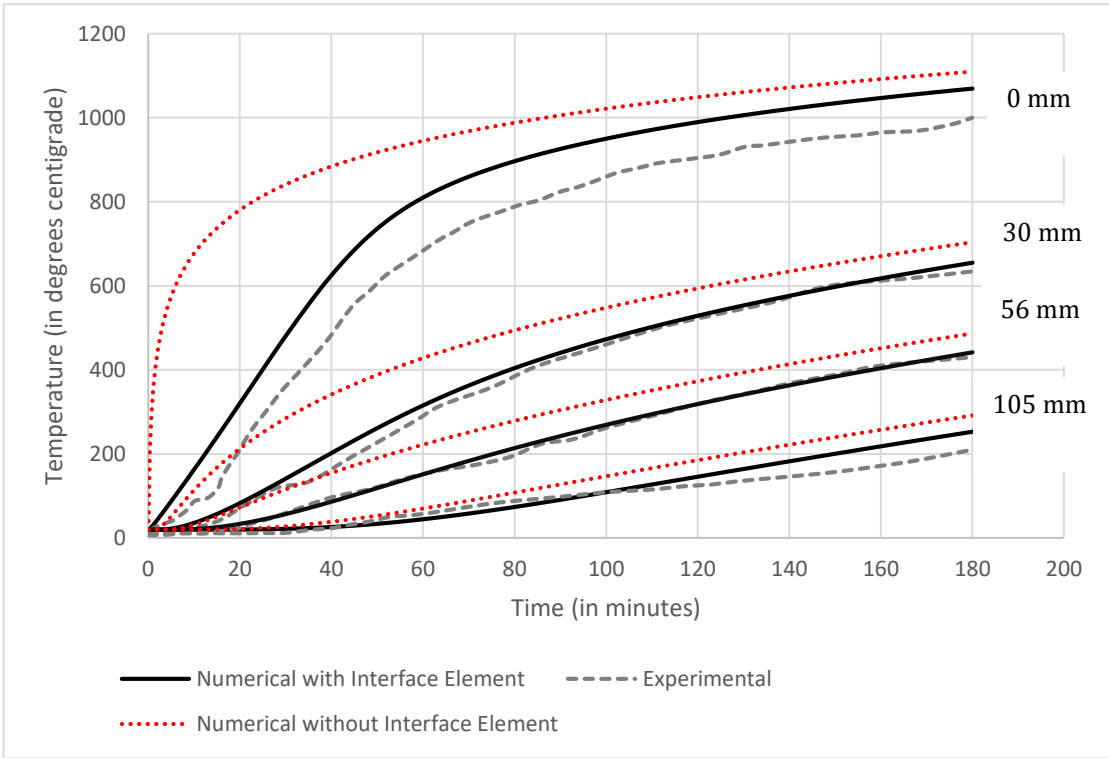


Figure 5.8 Temperature distribution for emissivity of steel as 0.5

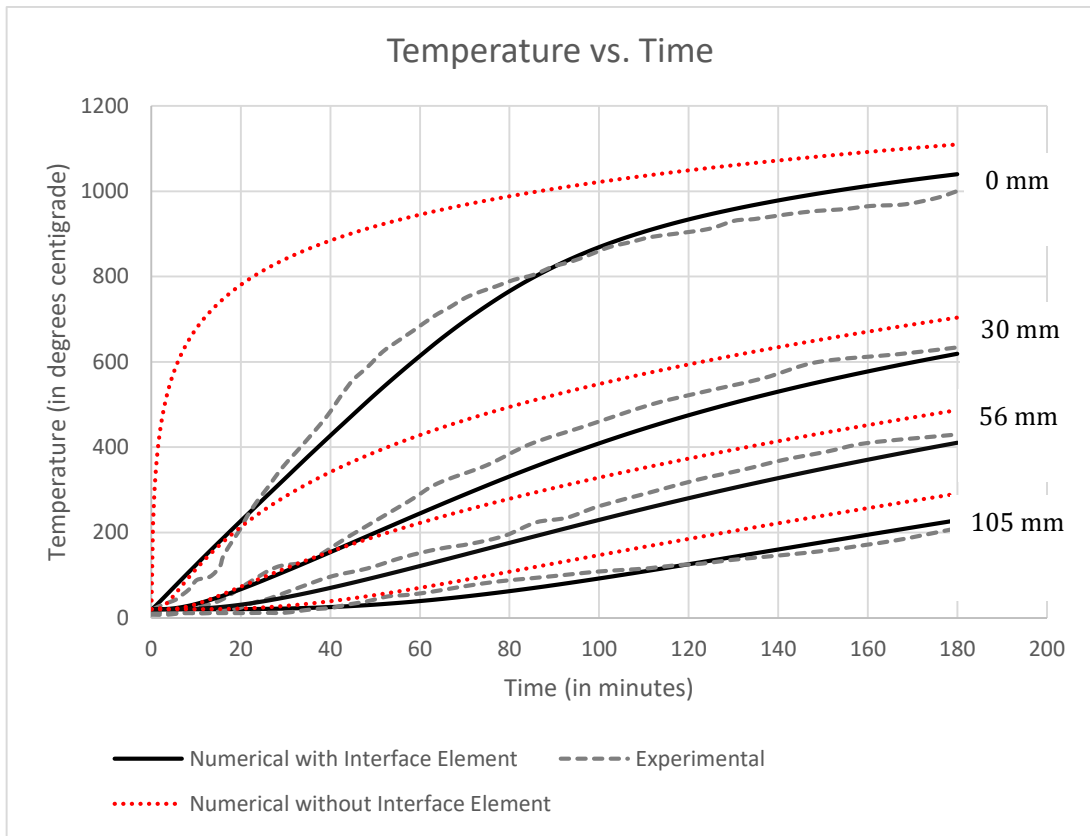


Figure 5.9 Temperature distribution for emissivity of steel as 0.3

5.4 Results: TrayDec Slab

The numerical results are compared with the experimental values and are shown below:

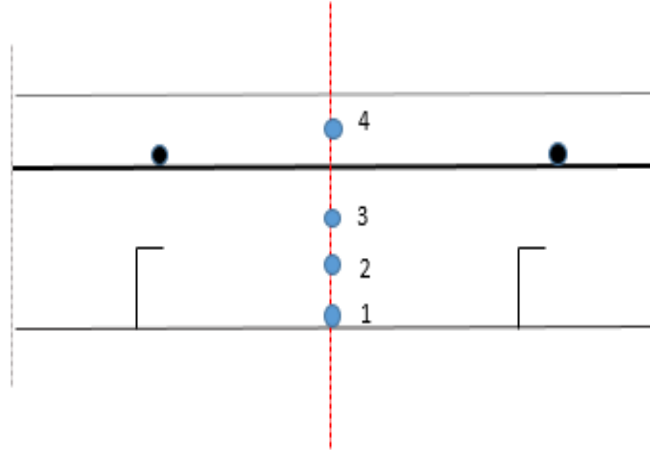


Figure 5.10 Position of Temperature Calculation for TrayDec Slab

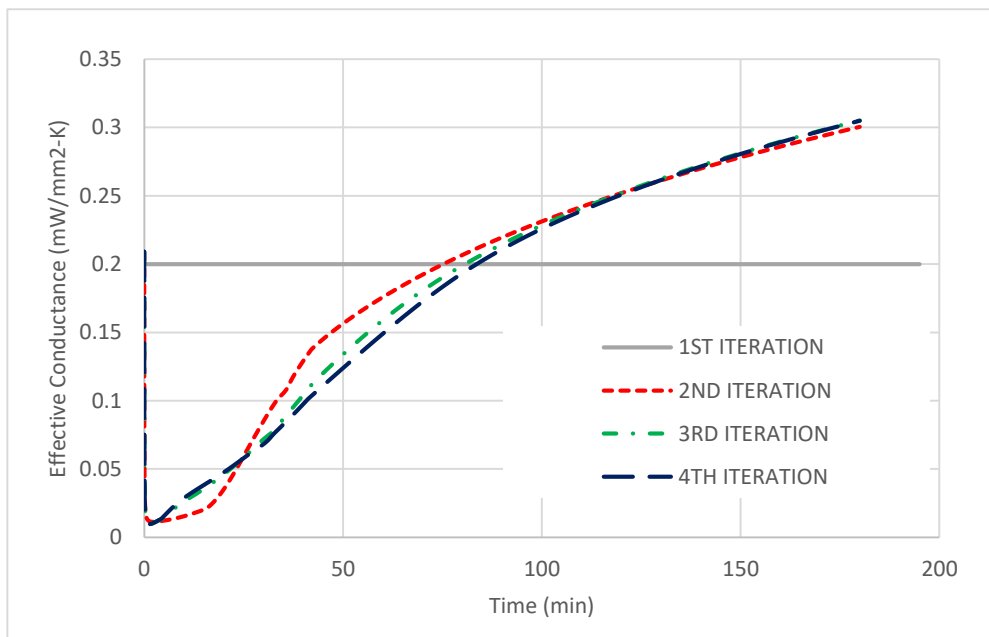


Figure 5.11 Effective Conductance vs. Temperature

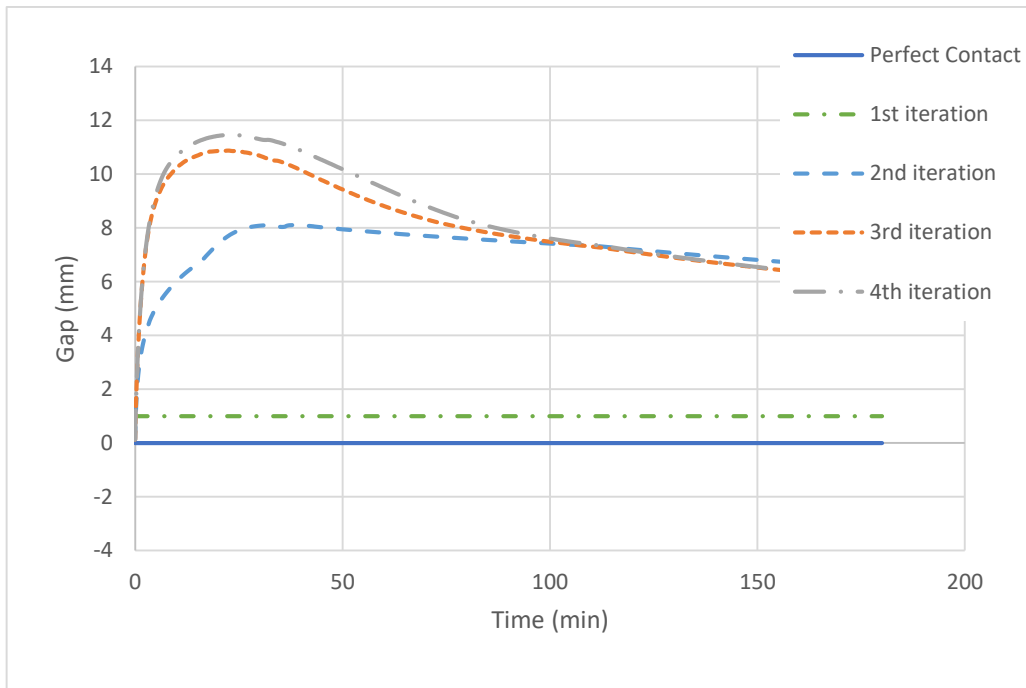


Figure 5.12 Average Gap vs. Temperature - Traydec slab

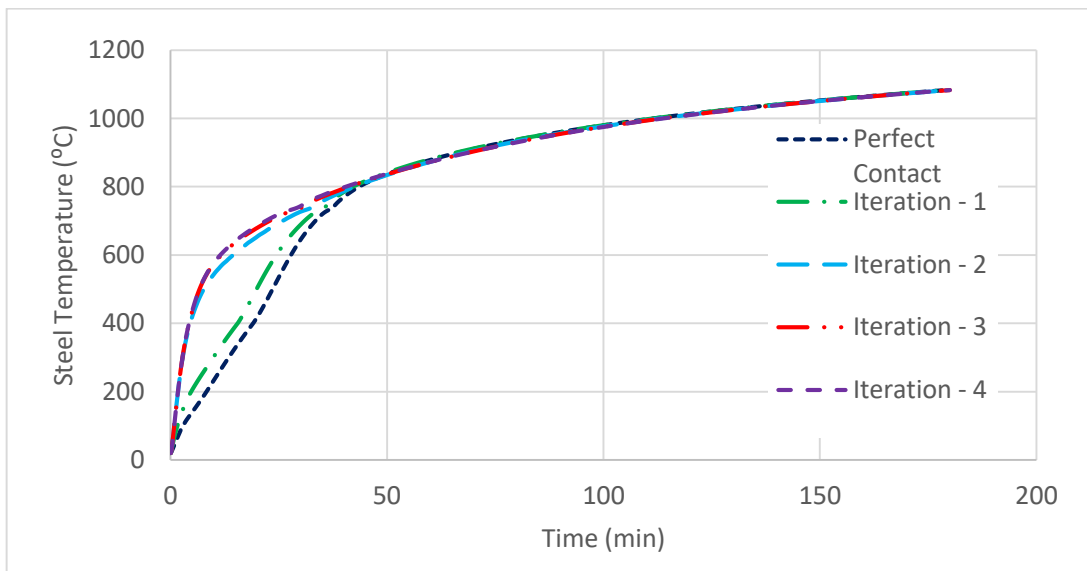


Figure 5.13 Variation of Steel Temperature - Iterative Procedure

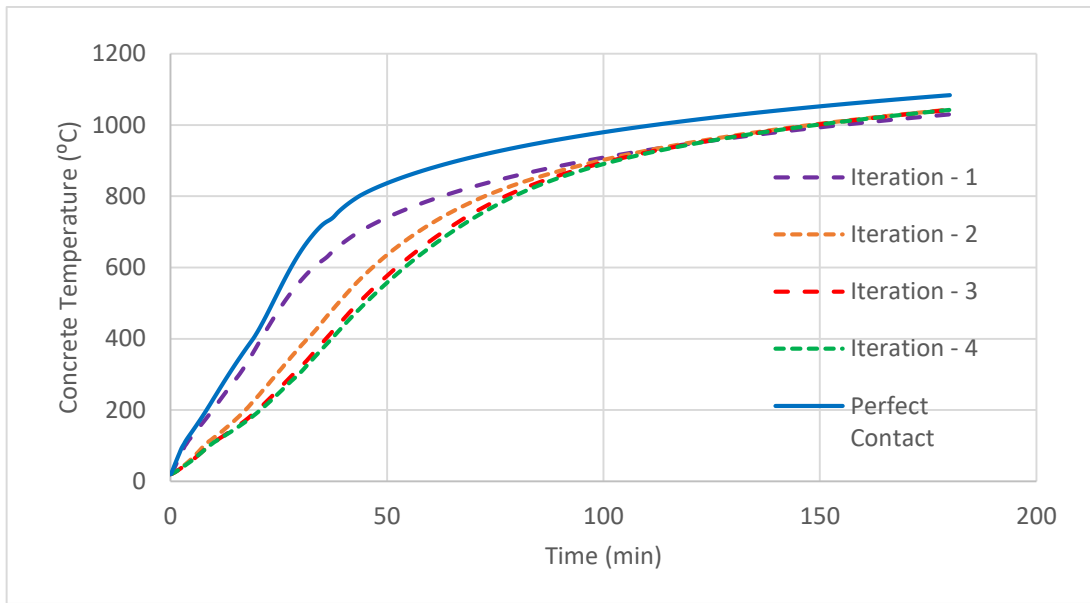


Figure 5.14 Variation of Concrete Temperature - Iterative Procedure

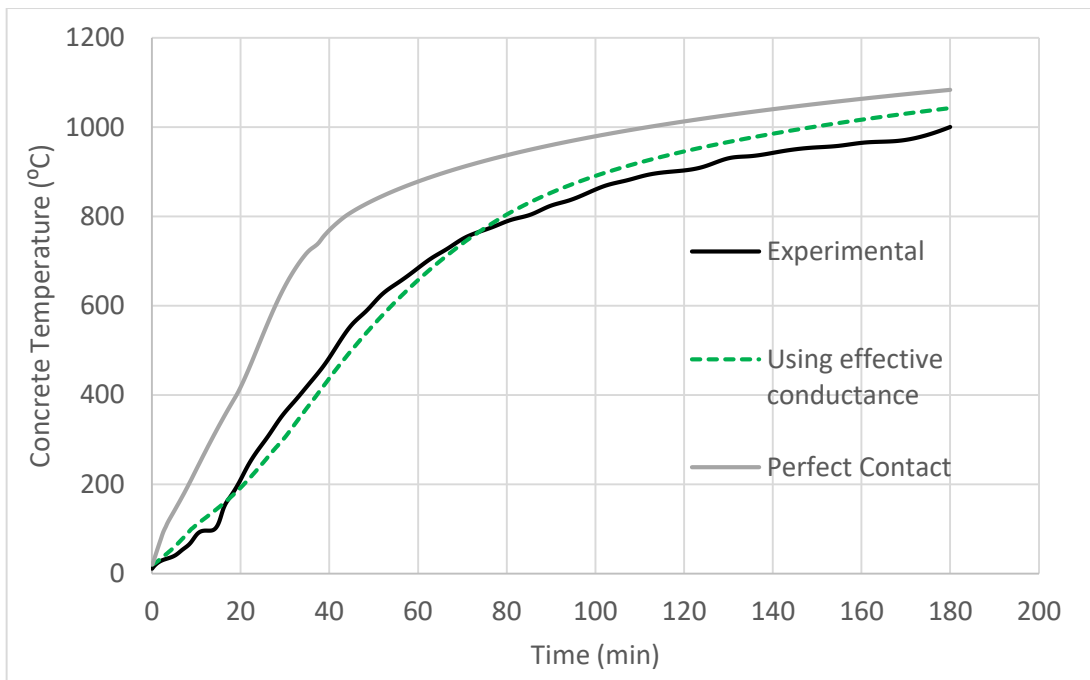


Figure 5.15 Comparison of Concrete Temperature with effective conductance and perfect contact

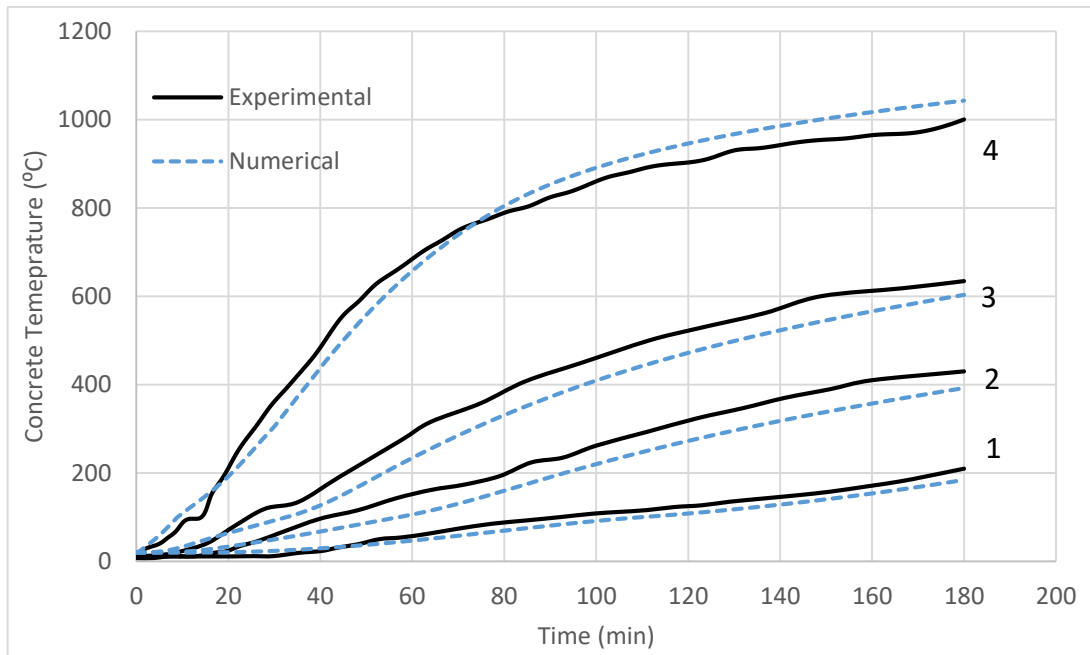


Figure 5.16 Temperature profile across the concrete section - TrayDec Slab

5.5 Results: Hibond Slab

The numerical results are compared with the experimental values and are shown below:

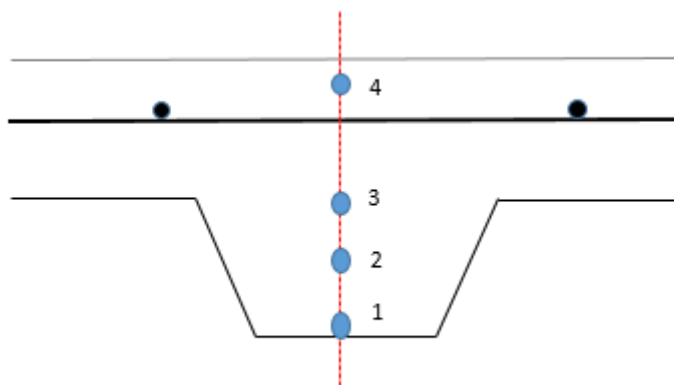


Figure 5.17 Positions of Temperature Calculations - Hibond Slab

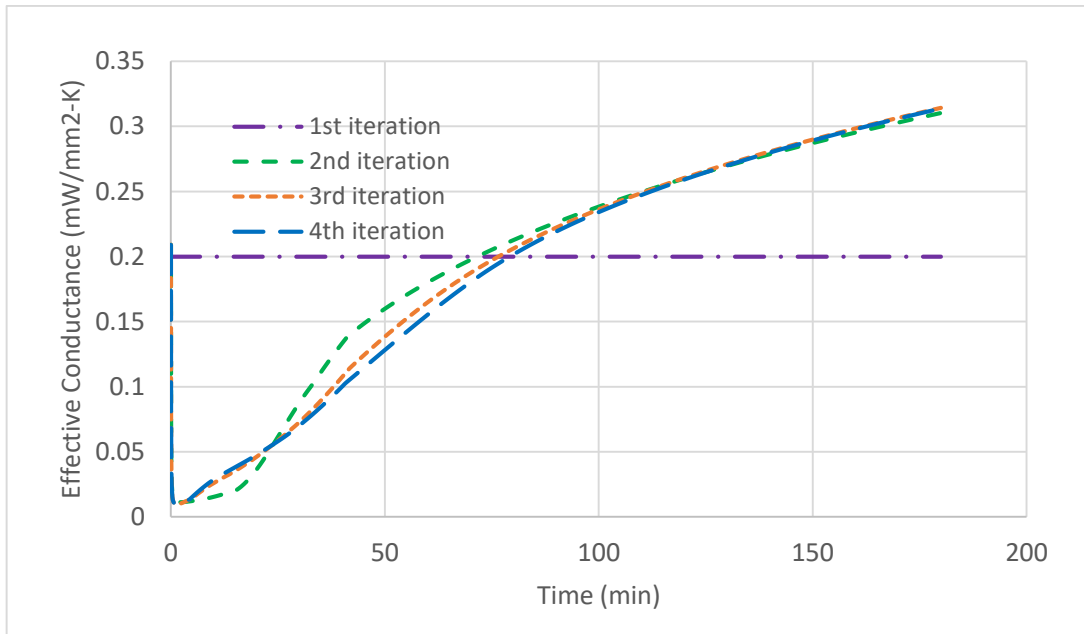


Figure 5.18 Effective Conductance vs. Temperature

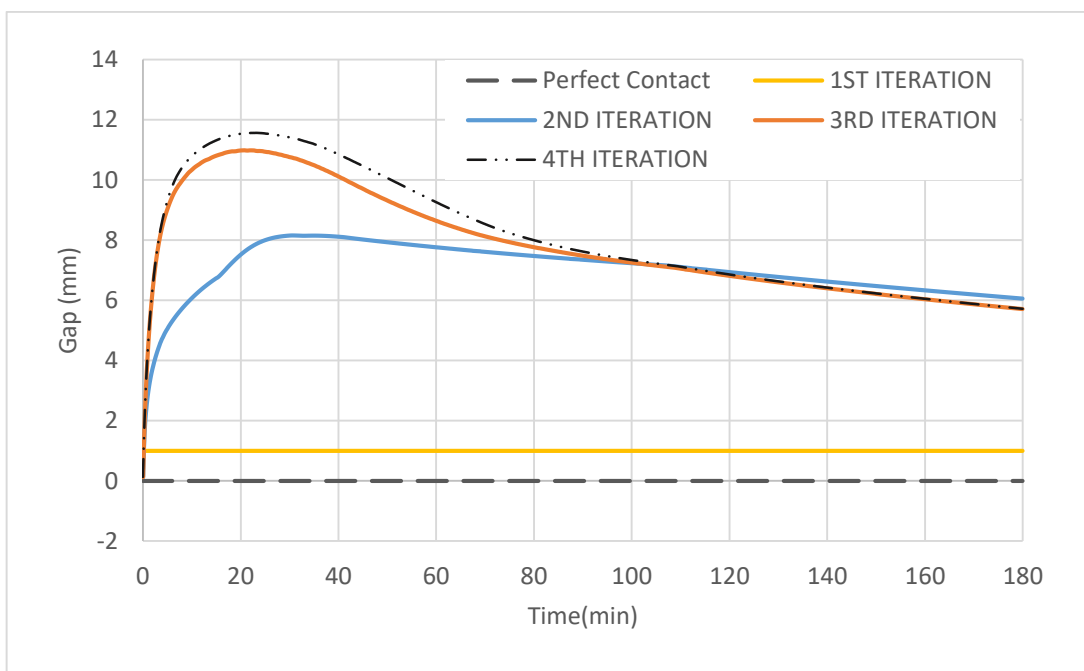


Figure 5.19 Average gap variation with temperature

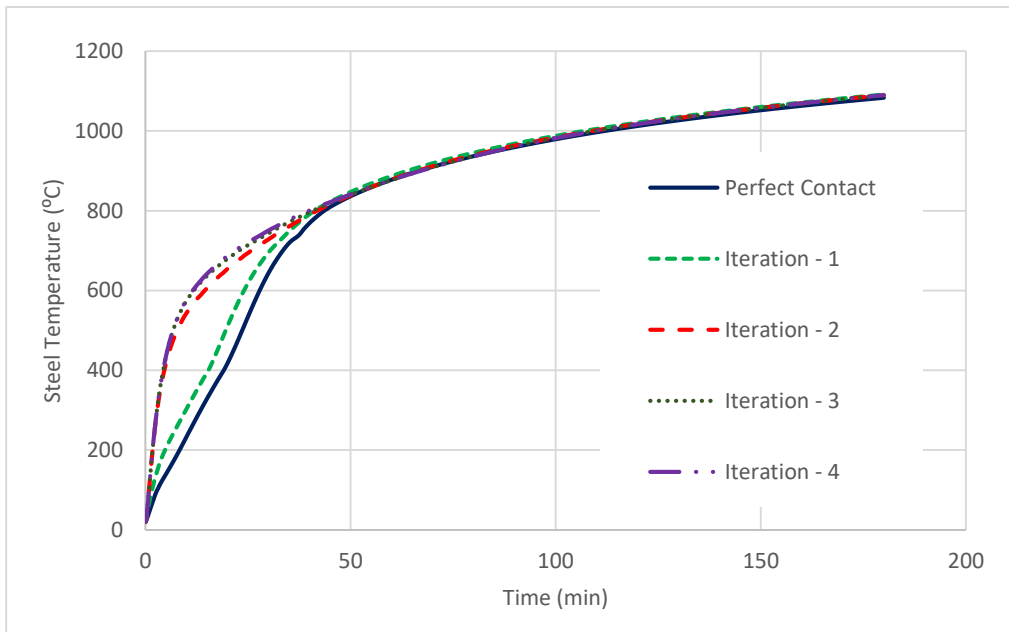


Figure 5.20 Variation of steel temperature - Iterative Procedure

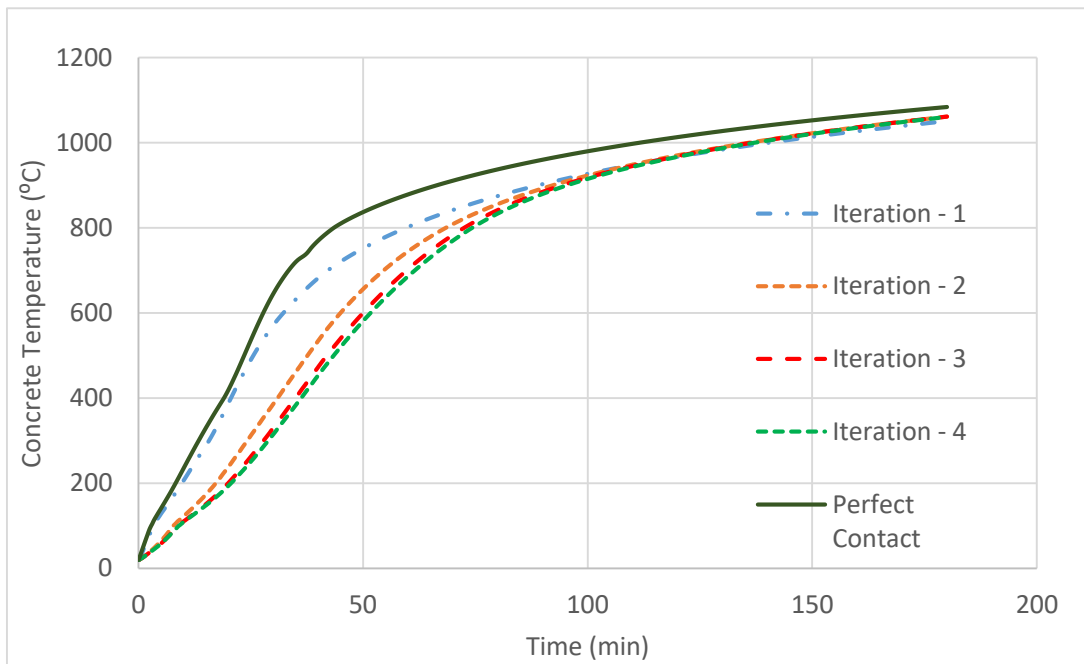


Figure 5.21 Variation of Concrete Temperature

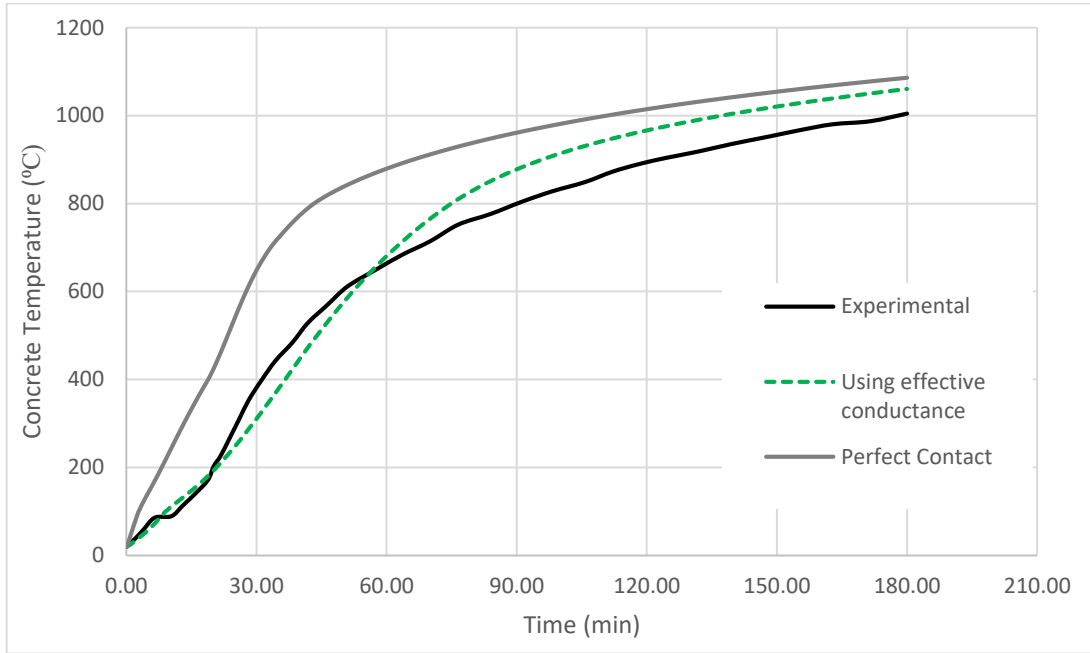


Figure 5.22 Comparison of Concrete Temperature With effective conductance and perfect contact

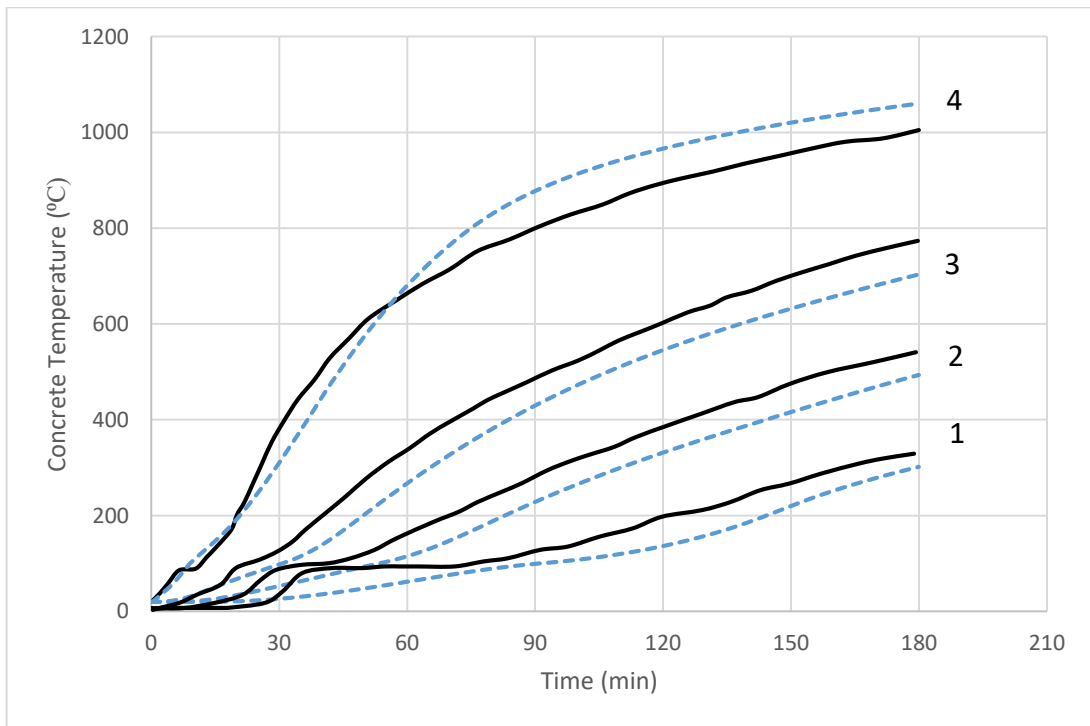


Figure 5.23 Temperature profile across the concrete section - Hibond Slab

5.6 Conclusions

From the above study, it is verified that the numerical results are over predicted when there is a perfect contact is assumed between the steel and concrete. Emissivity and view factor are the parameters which influence the equivalent conductance property, and indicate how good is the convergence of results of the numerical analysis when compared to the actual results. The proposed equation accounts for the debonding effect and using an interface element yields very good results and in turn better fire resistance prediction, but more experimental validation needs to be done. The iterative procedure using effective gap calculation proves to be a better way to tackle the insulation effect.

References

- [1] A.F. Hammerlinck (1991), “The behaviour of fire exposed steel-concrete composite slabs”, Ph.D. thesis, Eindhoven University of Technology
- [2] C.Both (1998), “The Fire Resistance of Composite Steel-Concrete Slabs”, Ph.D. thesis, Delft University of Technology.
- [3] J. Jiang, J.A. Main, F. Sadek, J.M. Weigand (2017), “Numerical Modelling and Analysis of Heat Transfer in Composite Slabs with Profiled Steel Decking”, Engineering Laboratory, National Institute of Standards and Technology, Technical Note 1958 <https://doi.org/10.6028/NIST.TN.1958>
- [4] L. Lim, Andrew Buchanan, Peter Moss, Jean Marc Franssen, “Numerical Modelling of Two Way Reinforced Slabs in Fire”, Engineering Structures 26 (2004), Pg. 1081-1091.
- [5] M.A.Halim, M.R.Hakmi, D.C. O’Leary (1999), “Fire Resistance of Composite floor slabs using a model fire test facility”, Engineering Structures 21, Pg. 176 – 182.
- [6] C. G. Bailey, S. Guo (2011), “Experimental behaviour of composite slabs during heating and cooling phases of fire”, Engineering Structures 33, Pg. 563-571.
- [7] S. Guo (2012), Experimental and numerical study on restrained composite slab during heating and cooling, Journal of Constructional Steel Research 69, Pg.95-105
- [8] EN 1992-1-2:2004, Eurocode 2 – Design of Concrete Structures Part 1-2: General Rules for Structural Fire Design
- [9] EN 1993-1-2:2004, Eurocode 3 – Design of Steel Structures Part 1-2: General Rules for Structural Fire Design
- [10] Linus Lim, Colleen Wade – Experimental Fire Tests of Two Way Concrete Slabs, Fire Engineering Research Report (02/2012)
- [11] Guo-Qiang Li, Nasi Zhang, Jian Jhang (2017), “Experimental Investigation on thermal and mechanical behaviour of composite floors exposed to standard fire”, Fire Safety Journal 89, Pg. 63-76